Synthesis and Characterization of α-Al_2O_3 by Sol-Gel Process and Development of Zn-Al_2O_3 Composites by Powder Metallurgy Route

A thesis submitted in partial fulfilment
of the requirements for the degree of

Master of Technology (Dual Degree)

in

Metallurgical and Materials Engineering

by

Aishwarya Rani Sahoo

(Roll no. - 710MM1096)

Under the supervision of

Dr. S.N Alam

Department of Metallurgical & Materials Engineering

National Institute of Technology Rourkela

Odisha, India

2015

Department of Metallurgical & Materials Engineering
National Institute of Technology Rourkela
Odisha, India

CERTIFICATE

This is to certify that the thesis entitled, **"Synthesis and characterization of α-Al_2O_3 by sol-gel process and development of Zn-Al_2O_3 composites by powder metallurgy route"** submitted by **Aishwarya Rani Sahoo (710MM1096)** in partial fulfilment of the requirements for the award of Master of Technology degree in Metallurgical and Materials Engineering at the National Institute of Technology Rourkela is a bonafide and authentic research work carried out by her under my supervision and guidance. To the best of my knowledge, the work embodied in this thesis has not been submitted earlier, in part or full, to any other university or institution for the award of any degree or diploma.

Dr. S.N Alam **Date:**
(Supervisor)
Department of Metallurgical & Materials Engineering
National Institute of Technology Rourkela

ACKNOWLEDGEMENT

I would like to express my sincere gratitude to **Prof. S. C. Mishra,** Head of the Department, Metallurgical and Materials Engineering, National Institute of Technology Rourkela for giving me an opportunity to work on this project and providing the valuable resources and facilities during the course of the work.

With great pleasure, I would like to convey my heartfelt gratitude and regards to my project supervisor **Dr. S.N Alam**, Department of Metallurgical and Materials Engineering, National Institute of Technology Rourkela, for his valuable guidance, constant encouragement and kind help throughout the project work and the execution of the dissertation work. An erudite teacher, a magnificent personality and a strict disciplinarian, I consider myself fortunate to have worked under his supervision.

I would also like to extend my sincere thanks to **Mr. Uday Kumar Sahu,** Department of Metallurgical and Materials Engineering, NIT Rourkela, for providing valuable insight and assistance during the experimental work. I am highly grateful to **Mr. Lailesh Kumar**, Research scholar, Department of Metallurgical & Materials Engineering, NIT Rourkela for showing me the guideline as well as rendering support and expertise needed for carrying out the work. I am highly indebted towards **Mr. Deepankar Panda, Mr. Deepanshu Verma and Ms. Pallabi Bhuyan** for their continual guidance and support. I would like to convey my sincere gratitude to **Mr. Kishore Kumar Mahato** and **Mr. Rajesh Patnaik** for rendering support while conducting experiments.

Last but not the least; I would like to express my profound gratitude and indebtedness to my parents and friends for their constant motivation, support and encouragement.

Aishwarya Rani Sahoo **Date:**

Metallurgical and Materials Engineering Department

National Institute of Technology Rourkela

CONTENTS

List of Figures

List of Tables

Abstract

In the present study α-Al_2O_3 powders of nanometric size were successfully synthesized by sol-gel method using two different precursors, one using aluminium chloride($AlCl_3$), ethanol(C_2H_5OH) and ammonia(NH_3) followed by calcination at 1200^oC for 2 h in a furnace, and the second process using aluminium nitrate ($Al(NO_3)_3$), malic acid ($C_4H_6O_5$) and polyvinylpyrrolidone, PVP ($(C_6H_9NO)_n$) followed by heat treating at 1250°C for 2 h. The alumina formed were analysed by X-ray diffraction (XRD) and particle size analysis to characterize the powders in terms of their crystallinity and their crystallite size. Further characterizations of particles were carried out using scanning electron microscopy (SEM), high resolution transmission electron microscope (HRTEM), differential scanning calorimetry (DSC) and Fourier transform infrared spectroscopy (FTIR) techniques. It was found that much finer particle size of α-Al_2O_3 could be achieved when $Al(NO_3)_3$ was used as a precursor. The decrease in size accompanied by an increase in aspect ratio makes it an ideal reinforcing agent for high strength composites and results in its highly superior properties. The present study also involved the development of Zn-Al_2O_3 composites by reinforcing the Zn-matrix with α-Al_2O_3 as reinforcement. α-Al_2O_3 is very attractive due to their unique combination of excellent mechanical properties and high thermal stability which makes them an ideal reinforcing agent for high strength composites. Zn-Al_2O_3 composites were developed containing 50 and 60 vol.% α-Al_2O_3 by an ex-situ process that includes blending commercially available Zn and α-Al_2O_3 powders together in required compositions followed by compaction at 300 MPa and heat treatment at 500^oC for 2 h. The Zn-Al_2O_3 composites fabricated were analysed by using optical microscopy, SEM and EDX. Mechanical properties like wear resistance and hardness of the composites were analysed to find out the effect of the addition of α-Al_2O_3 in the Zn-matrix. It was found that addition Al_2O_3 to Zn matrix improved the hardness as well as the wear resistance of Zn.

Keywords: Sol-gel, α-Al_2O_3, Zn-based metal matrix composites, Wear

CHAPTER-1

INTRODUCTION

1.1 Background of the Present Investigation

There is a dire need of new materials with special combination of properties to cater to the needs of modern technology. Nanotechnology provides the most effective solution to such a problem as a result of development of nano-structured materials with incredibly unique combination of properties as well as versatile applications. Ceramics embedded in metal matrix profoundly alter the mechanical, thermal and physical properties and result in a wide range of potential applications (thermal barrier coatings, structural components, fire resistance etc). The properties of a MMC are strongly dependent on the properties of reinforcing agents, volume fraction, distribution and interfacial area of reinforcements.

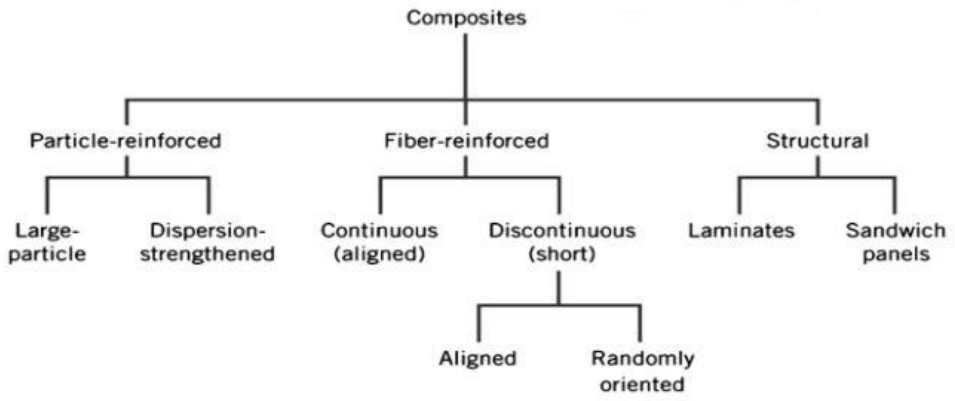

Figure 1.1 Overview of types of composites

The transition from micro size to nano size results in a large number of changes in physical properties. The most important ones are the enhancement in the ratio of surface area to volume and the size of the particles where quantum mechanics is predominant. [1] The increase in the ratio of surface area to volume results in an increasing superiority of the behaviour of atoms on the particle surface than those in the interior. This in turn affects the properties of the particle as well as its interaction with other materials. The very high surface area of the nano particles are responsible for the high performance of these materials in various fields like electronics, optics, biomedical implants, as effective reinforcements in composites etc. This also results in increase in strength, enhanced heat and chemical resistance. Nano particles have attracted a lot of attention in past few years due to their excellent mechanical, physical, optical and chemical properties that make them unique and different from bulk material properties since the uniformly distributed, ultra fine particles have considerable unique properties such as high resistance to oxidation, high resistance to crack propagation and extremely high strength. Having dimensions below the critical

wavelength of light that subsequently renders them transparent, these particles are useful for applications like coatings, electronic devices etc. metal oxide or ceramic nano powders such as titanium, zinc, aluminium and iron oxides are widely used.

As a result of unique combination of incredibly high mechanical properties and superior thermal stability, nanosized alumina has attracted a lot of research and development. The unique concoction of morphology, structure, dimensions create a plethora of superior properties like enhancement in hardness, crack propagation resistance, wear resistance etc thereby them ideal for reinforcing purposes in high strength composites. These excellent properties of nano-sized alumina makes it ideal to be used in biomedical engineering, optical devices, coatings against corrosion, high temperature materials, for fabrication of sensors , fuel cells etc.

1.2 Scope and Objective of the work

Alumina nanopowders have the potential to be utilized as material for biocompatible implants. It is an inert biomaterial and is also biodegradable. The synthesis of alumina by sol-gel method has been reported by several researchers using different precursors. The sol-gel method is known to be an alternative route for the synthesis of ceramic powders. The present study deals with the synthesis and characterization of Al_2O_3 using two different precursors. In the first method inorganic aluminum chloride, $AlCl_3$ was used. Whereas in the second method aluminium nitrate, malic acid and poly vinyl pyrrolidone (PVP) was used.

Alumina is one of the most widely used ceramic reinforcements and is highly economical. It is found in a number of phases out of which α-Al_2O_3 is the most stable. This in turn results in high temperature stability, good compressive strength and very good wear resistance properties. High coefficient of thermal expansion and low thermal conductivity are its major drawbacks. Al_2O_3 (3.95gm/cc) is almost half as light as Zn (7.14 gm/cc). As a result during liquid phase sintering Al_2O_3 floats in Zn. Al_2O_3 is a ceramic. The low melting point of Zn(419.6^oC) restricts its use in high temperature applications. [2] The present study involves the preparation of Zn-Al_2O_3 composites by an ex-situ technique. In the present study soft Zn metal matrix was reinforced with hard Al_2O_3 ceramics particles resulting in enhanced physical and mechanical properties of the composite thus formed. [3]

CHAPTER-2

LITERATURE REVIEW

2.1 Alumina (Al_2O_3)

Commonly known as alumina, aloxite or alundum in the mining, ceramic and materials science industries, aluminium oxide (Al_2O_3) is a pale white or almost colourless crystalline substance. It is basically aluminium (III) oxide and is one of the common forms of aluminium oxide that is used so widely. The major naturally occurring ore of Alumina is bauxite and it contains variable amounts of hydrous (water-containing) aluminium oxides. Usually found in nature in the form of the minerals corundum, ruby and sapphire, it is in fact a crystalline polymorphic phase α-Al_2O_3. Being amphoteric in nature, Alumina or aluminium oxide possesses the ability to react with acids as well as bases.

2.1.1 Polymorphs of Alumina

The property of a material to exist in more than one form in nature is known as polymorphism. Alumina has several polymorphs including γ, θ, and α, the most common being the α-Al_2O_3. The α structure is the most stable one among its other polymorphs and finds a lot of applications, but nevertheless the metastable phases like γ and θ also appear during phase transitions and reactions. The properties of the different polymorphs are different and hence have different applications in various fields. But the resultant of all transformation phases is α-Al_2O_3 phase at high temperature.

2.1.2 Properties of alumina

Table 2.1 Properties of alumina

Crystal structure	Trigonal
Molar Mass	101.96 g. mol^{-1}
Density	3.95-4.1 g /cm^3
Melting point	2072^oC
Boiling point	2977^oC
Thermal conductivity	30$W.m^{-1}. K^{-1}$
Electrical resistivity	$1x10^{14}$ to $1x10^{15}$ Ω.cm
Tensile strength	69 to 665 MPa
Compressive strength	690 to 5500 MPa
Mohs hardness	9
Bulk modulus	137-324 GPa
Shear modulus	88-165 GPa
Young's modulus	215-413 GPa

2.1.3 Application of Alumina

- Composite fiber-It is used as reinforcing agents to develop high-performance materials
- Filler-Due to its inertness and pale white color, it is a favoured filler for plastics, cosmetics etc.
- Catalysis-It acts as a catalyst as well as a catalyst support in various industrial reactions like Claus process and Ziegler-Natta polymerizations etc.
- Purification-It is used for purifying gas streams
- Abrasive-Known for its excellent hardness and strength, it is commonly used in grinding operations, polishing and coating purposes
- Paint- Alumina flakes are used widely in paint and for decorative effects in the automotive or cosmetic industries.
- Other applications include medical prosthesis, laser tubes, seal rings, electronic substrates, electrical insulators, wear components, thermocouple tubes etc.

2.1.4. Alumina Synthesis Techniques

α-Al_2O_3 can be synthesized by various synthesis routes which are as follows:

- Flame aerosol method
- Chemical vapour deposition (CVD)
- Electrospinning
- Spray pyrolysis method (polymer pyrolysis)
- Sol-Gel method

In this present investigation, we have used the sol-gel process taking two different precursors in order to synthesize α-Al_2O_3. [4]

2.2 Sol-gel Process

The Sol-gel process, popularly known as chemical solution deposition, has a wide range of applications in ceramics and materials science.

The process consists of the following steps:

- Stable sol formation using precursors
- Formation of a gel by adding suitable reagent
- Allowing the gel to mature and age into a solid mass
- Removal of any remaining liquid phases by drying the gel

- Calcination of the mass formed in a furnace at a high temperature

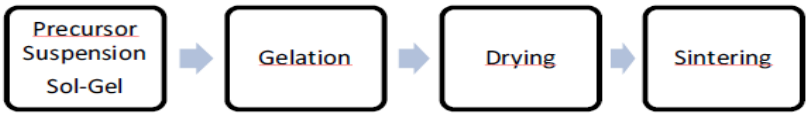

Figure 2.1 Schematic representation of the Sol-gel process

Sol-gel technique is a continuous and simple process involving low cost and high yield. The advantages of this method include obtaining high purity materials, process versatility, ease of synthesizing special materials and saving energy by using low operation temperatures.

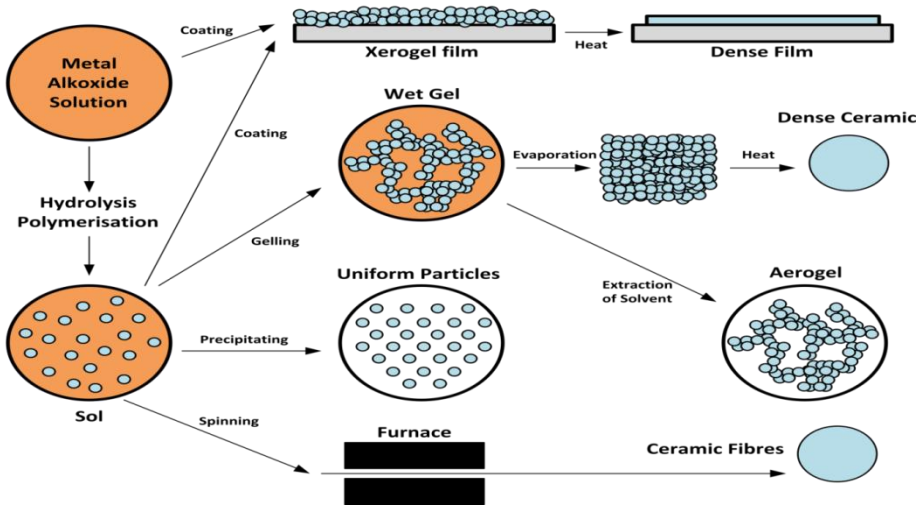

Figure 2.2 Various Sol-gel techniques and their products

2.3 Alumina (α-Al_2O_3) as Reinforcement

The most important objective of reinforcement in a composite is to enhance the mechanical properties of the system. Different fibers posses different properties and hence they all affect the overall properties of the composite produced in various ways. The fiber is used to carry the load of the composite. Ceramic fibers have high strength and elastic modulus with high temperature capability and are suitable as high temperature structural materials. Al_2O_3 finds applications as a reinforcing agent in a wide range of metal matrix composites (MMCs). It enhances the rigidity and decreases the rate of crack propagation. [5] These alumina fibers embedded in a matrix can greatly aggravate the composite's overall properties. [6]

2.4 Composites

Composite materials or composites are materials made from a combination of two or more constituent materials which have properties that are different physically, chemically, or in both ways. [7] The individual components however maintain their identity and remain distinct in the finished product. The two constituent materials, in the final composite, are separated by a distinct interface. The constituent materials used in making the composite form two phases- the reinforcing phase and the matrix phase. The mechanical properties of the composite are improved by the addition of the reinforcing phase in the matrix phase. The matrix materials that are used for composites can be metal, ceramic or polymer. The reinforcing phases are added in the form of particulates, fibres, sheets, etc. Selection of a proper reinforcement and a matrix can lead to enhancement of properties such as strength and stiffness along with low density. [8-9]

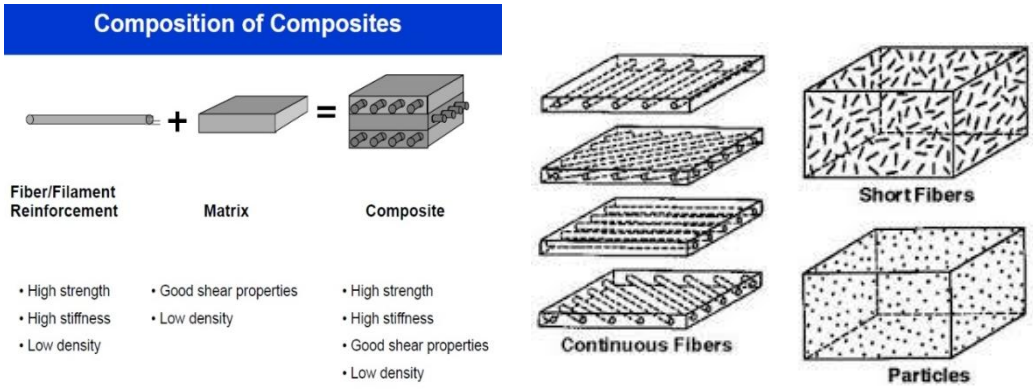

Figure 2.3 (a) Constituents of a composite (b) Types of reinforcements

The properties of composites are as follows:

- Light weight
- Improved fatigue strength
- Improved stress-rupture life
- High specific strength and stiffness
- High toughness (impact and thermal shock resistance)
- Greater hardness and Corrosion resistance
- Low coefficient of thermal expansion
- High strength at elevated temperatures

2.5 Application of Composites

Composites are of increasing importance due to their advanced properties and highly improved performance and hence they find applications in diverse fields such as:

- Automobile parts
- Aircrafts
- Bulletproof jackets
- Boat hulls
- Sport's kits
- Building constructions

2.6 Classification of Composites

Composites can be classified in two ways:

- On the basis of matrix
- On the basis of reinforcement

2.6.1 On the Basis of Matrix

The matrix phase is the continuous, ductile and less hard phase of a composite. It is responsible for holding the reinforcement and sharing its load. [10] On the basis of matrix, composites can be classified as follows:

2.6.1.1 Ceramic Matrix Composites (CMCs)

It comprises of a ceramic matrix reinforced with ceramic materials (oxides, carbonates etc.) as the dispersed phase. However in ceramic matrix composites, fibre components that can withstand relatively higher temperatures required for ceramic production can only be used. The fibre materials should also have creep resistance and resistance to oxidation.

2.6.1.2 Polymer Matrix Composites (PMCs)

It comprises of a polymer matrix pooled with fibrous reinforcement. [11] Polymer matrix composites (PMCs) contain a wide range of short, discontinuous or continuous fibres bound together by a polymer. Their cost of production is low and they have simple fabrication methods**.** [10] The reinforcement in a PMC account for the high stiffness and strength of the composite. The composite is so designed in order to enable the reinforcement to support the mechanical loads subjected to the structure in service. The matrix binds the fibers together keeping them in place and transfers loads between them.

2.6.1.3 Metal Matrix Composites (MMCs)

It consists of a metal matrix combined with either a ceramic or a metal dispersed phase. The matrix is usually a lighter metal (Aluminium, Magnesium, etc.) in case of structural

applications. In case of high temperature applications, the matrix could be cobalt or cobalt nickel alloys.

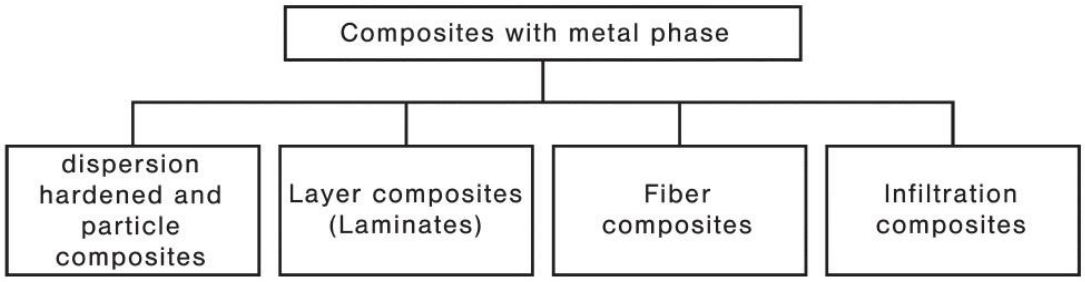

Figure 2.4 Classification of composite materials with metal matrices

- Advantages of MMC over polymer matrix composites (PMCs)
  a) High operating temperatures
  b) Non-flamability
  c) Greater resistance to degradation
- Disadvantages
  a) They are costlier than PMCs

2.6.2 On the Basis of Reinforcement

The secondary phase or the reinforcement is embedded in the matrix phase. It is called the reinforcement because it is stronger than the matrix phase. The reinforcement is not just used for strengthening purposes but it can also change other physical properties such as friction coefficient, wear and abrasion resistance, or thermal conductivity. The composites can be classified on the basis of reinforcement in three ways:

2.6.2.1 Particulate Composites

It consists of tiny particles of one material embedded in another. The can be very small particles of size less than 0.25 microns, platelets, chopped fibers or hollow spheres. The matrix acts as the binding material for structural use and the reinforcement provides the desired material properties. The particle reinforcement may either be randomly distributed or may have preferred orientation such as two dimensional flakes laid parallel to one another.

Some major applications of these kinds of composites are in wood particle boards and in concrete where sand particles are bound together by a mixture of water and cement.

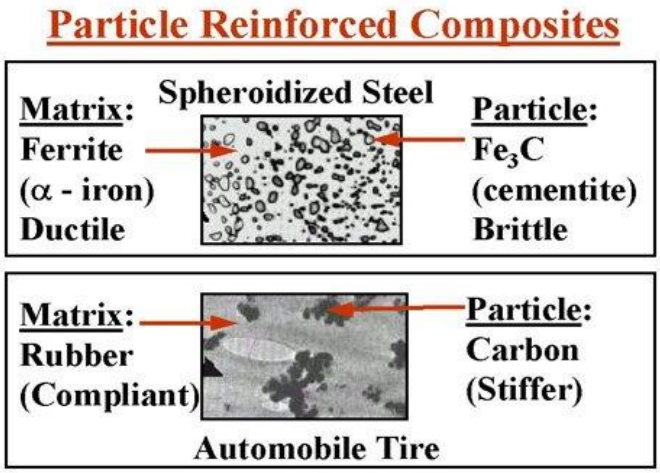

Figure 2.5 Particle reinforced composites

2.6.2.2 Fiber Reinforced Composites

Dispersed phase having discontinuous fibres having are called short-fibre reinforced composites, whereas a dispersed phase in form of continuous fibres is called long-fibre reinforced composites. One major application of these composites is in making bulletproof vests in which crisscross system of fibers is used. A fibre-reinforced composite (FRC) is a composite building material that consists of three components.

- The fibres as the discontinuous or dispersed phase
- The matrix as the continuous phase
- The fine interphase , also known as the interface.

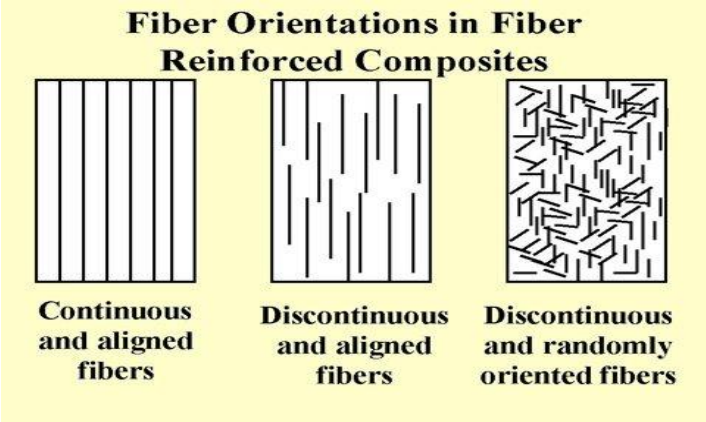

Figure 2.6 Fibre orientations in fibre reinforced composites

2.6.2.3 Laminate Composites

A fibre reinforced composite consisting of several layers with different fibre orientations is called multilayer composite**.** Laminated Composites are made up of panels or sheets which are two dimensional in nature. The layers are arranged such that in each successive layer the orientation of the direction of high strength changes**.** These are widely used in space shuttle heat panels.

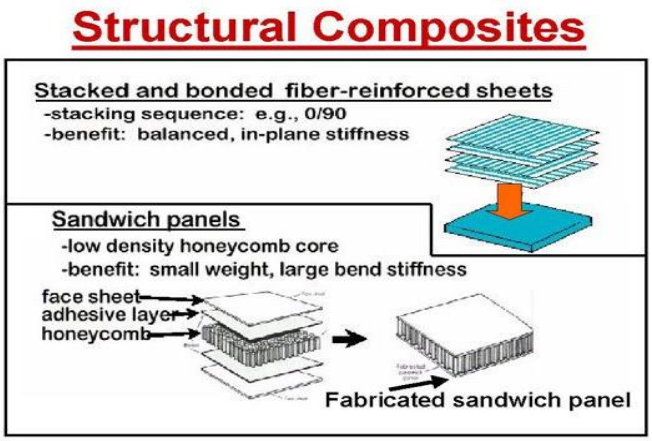

Figure 2.7 Laminate composite structure and fabrication

2.7 Synthesis of Metal Matrix Composite

Metal matrix composites use typical commercial alloy metal for matrix materials e.g. Aluminium, Titanium etc. Besides improving specific strength and stiffness, they also posses damping properties. Metal matrix composites can be synthesised in the following ways:

2.7.1 Solid State Fabrication

In this process, the bonding between the matrix and the reinforcement takes place through diffusion at elevated temperature and pressure. There are mainly 3 ways for the fabrication of MMC by solid state route:

- Hot Pressing Fabrication
- Hot Isostatic Pressing Fabrication
- Hot Powder Extrusion Fabrication

2.7.2 Liquid State Fabrication

In this process the dispersed phase is incorporated into molten metal matrix, followed by solidification. For higher level of mechanical properties, good wetting between the dispersed phase and the matrix phase is very important. [12] The reinforcement is generally coated for good wettability. The added advantage of coating is that it prevents chemical interactions between the two phases.

There are many methods for the preparation of MMC by liquid fabrication route:

- Pressure Die Infiltration
- Stir Casting
- Gas Pressure Infiltration
- Infiltration
- Squeeze Casting Infiltration

2.7.3 Sintering

In this method of fabrication, metal matrix and dispersed phase are both taken in the form of particles (generally powders) for successive condensing in solid state. The temperature used is just below the melting point of the metal, where diffusion takes place. Two major things happen during sintering, one is atomic diffusion occurs that leads to growth of welded areas, and the other is recrystallisation followed by grain growth that lead to decrease in porosity.

2.7.3.1 Sintering Atmosphere

The sintering process requires dire conditions and is usually carried out under protective atmospheres and at temperatures between 60 and 90% of the melting-point of the metals or alloys involved. [13] This is so in order to prevent oxidation of the large exposed surfaces and to enhance the reduction of surface oxides formed. The most common atmospheres used are of cracked ammonia, dry hydrogen, and partially combusted hydrocarbons.

2.7.3.2 Types of Sintering

- **Solid state sintering**

This involves only solid phases during sintering

- **Liquid Phase Sintering**

This involves the presence of some liquid phase at the sinter temperature

- **Reactive sintering**

This involves the reaction between particles to form new product phases

2.7.3.3 Special Sintering processes

The combination of consolidation and sintering along with high pressure results in a lot of special sintering processes which are as follows:

- Hot isostatic Pressing (HIP)
- Hot Rolling and Extrusion
- Hot pressing
- Pulse Plasma Sintering
- Spark Plasma sintering

- Spray deposition
- Hot Forging of Powder Preform

2.7.3.4 Stages of Sintering

- First Stage

Before sintering, the particles are just in contact with each other and as temperature is increased the additives starts to burn out.

- Second Stage

In this stage as the mobility of the atoms in particles increases, the rough surfaces of the particles gets smoothened and neck formation starts to occurs

- Third Stage

This stage is marked by the evolution of necks and grain boundaries resulting in densification and decrease in porosity [14]

- Fourth Stage

This stage is marked by the growth of grains and break out of the pores to form closed isolated spherical bubbles.

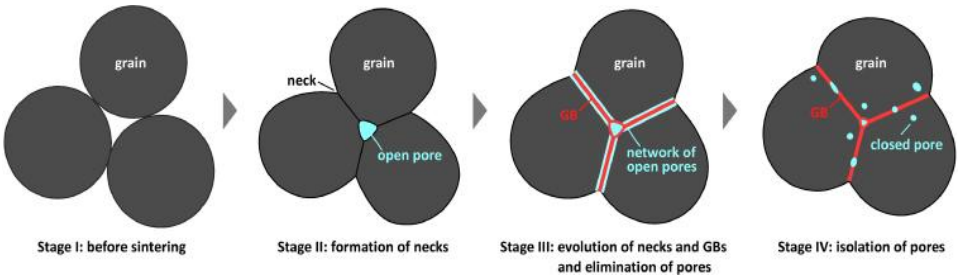

Figure 2.8 Different stages of sintering

2.7.3.5 Advantages of Sintering

- High purity and uniform materials can be developed
- Better control over grain size
- Absence of inclusions and segregated particles
- No requirement for deformation to produce directional elongation of grains

2.8 Zn and Zn-α-Alumina Composites

Zinc (Zn) is bluish-white in colour and has a highly lustrous surface finish. It is brittle at room temperatures but malleable at higher temperatures, i.e. around 100 to 150^{o}c. Most zinc production is from sulphide ores which are roasted to form zinc oxide (ZnO) which is further reduced by carbon to give zinc metal. A large portion of all zinc is used in order to galvanise metals like iron so as to prevent corrosion. The numerous properties of zinc are listed in the table below:

Table. 2.2 Various properties of Zinc (Zn)

Crystal structure	Hexagonal close-packed (HCP)
Molar mass	65.38 g. mol^{-1}
Density	7.14 gm/cm^{3}
Melting point	419.53^{o}C
Boiling point	907 ^{o}C
Young's modulus	108GPa
Electrical resistivity	59.0 nΩ.m(at 20^{o}C)
Thermal conductivity	116 W.m^{-1}. K^{-1}
Bulk modulus	70 GPa
Shear modulus	43 GPa
Mohs hardness	2.5
Brinell hardness	327-412 MPa
Poisson ratio	0.25

Zinc based alloys have found considerable applications due to their excellent flow properties, castability and excellent mechanical properties. But in spite of its attractive room properties zinc alloys show unsatisfactory results in performance due to their low melting point i.e. 419.53^{o}C. Hence by embedding or reinforcing the harder, stiffer and thermally stable alumina into the softer and ductile zinc, we can develop composites with highly improved mechanical properties.

Particle reinforced metal matrix composites (MMCs) are very important and have found special industrial applications in producing wear-resistance components. Zinc has a density of 7.14 gm/cc and the density of Al_2O_3 is 3.95 gm/cc. As Zn has a higher density compared to Al_2O_3 it is possible that Al_2O_3 floats in molten Zn whereas Zn remains at the bottom. Due to

better mechanical properties of Al_2O_3 the properties like hardness and resistance to wear could be better at the surface of the compact compared to inside of the compact. [15] As a result of the formation of fine and stable ceramic reinforcements in the metal matrix, the MMCs tend to exhibit enhanced mechanical properties. In the present investigation, Al_2O_3 reinforced Zn matrix composites with fibre volume % ranging from 50-60 % were manufactured by mixing and compaction followed by sintering process.

CHAPTER-3

EXPERIMENTAL DETAILS

3.1 Experimental Apparatus

3.1.1 Cold Uniaxial Hydraulic Press

This press makes use of a hydraulic cylinder to generate compressive forces. It is based on Pascal's principle which states that the pressure remains constant in a closed system. The system consists of a piston acting as a pump on a small cross-sectional area, as well as another piston with a larger area that generates a correspondingly large mechanical force. This is basically used to prepare green compacts which are later sintered in a tubular furnace. The blended samples were compacted using a under 300 MPa load by this machine. The press in use was designed by Soil lab and has a capacity of 1130 MPa.

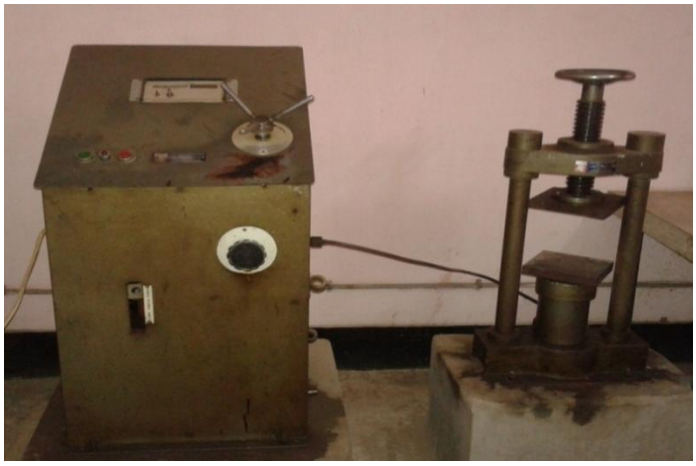

Figure 3.1 Uniaxial Hydraulic Press

3.1.2 High Temperature Horizontal Tubular Furnace

A tubular furnace is an electric heating device which consists of a cylindrical cavity covered by heating coils embedded in a thermally insulating matrix to carry out synthesis as well as purifications of various compounds. The temperature can be controlled by feedback from a thermocouple. The Zn and alumina compacts were sintered using this furnace in an inert atmosphere of argon gas at 500^{o}C for 2 h. Sintering is effective in reducing the porosity and enhancing properties such as translucency strength, thermal conductivity, strength and electrical conductivity etc. Sintering occurs through various stages starting from neck formation between particles to isolation of pores in the end. This vacuum and control atmosphere furnace is a product of Naskar & Company and can attain a maximum temperature of 1750^{o}C.

Figure 3.2 Horizontal Tubular Furnace

3.1.3 Particle size analyzer

The major working principles of a particle size analyzer depend on the optic properties of diffraction and scattering. Here diffraction and scattering phenomenon takes place as a beam illuminates the particles dispersed uniformly in the liquid. A large series of light rings are formed on the focal plane of the fourier lens when the diffracted or scattered light rays are passed through it. The radius of these light rings is related to the size of the particles whereas the density of light is given by number of particles. The particle size distribution of the sample is thus obtained. In this study, a MALVERN particle size analyzer was used to find out the distribution of particle size in the powder.

Figure 3.3 MALVERN Particle size analyzer

3.1.4 X-ray Diffractometer

X-ray diffractometers basically contain three elements which are an X-ray tube, a sample holder, and an X-ray detector. The heating of a filament contained in a cathode ray tube generates free electrons which when bombarded with the target material generates x rays.

Electrons with sufficient energy knock out the inner shell electrons of the target material, thereby producing characteristic X-ray spectra. In this work, the phase structure was identified by x-ray diffraction using Cu K_α(λ = 1.5406 Å) radiation. A Phillips X'pert Pro high-resolution X-ray diffractometer was used with a voltage of 30KV and current 20 mA

Figure 3.4 Phillips X'pert Pro high-resolution X-ray diffractometer

3.1.5 Optical Microscope

The optical microscope is a type of microscope that utilises visible light and a system of lenses in order to enlarge or magnify images of small objects. There are diverse ranges of optical microscopes and they can range from being extremely simple and basic to highly complex ones which aim to improve resolution and image contrast. The image from this kind of microscope is captured by light-sensitive cameras to generate optical micrographs. Its principle is similar to a simple lens system for magnifying small objects. In this research work, Zeiss AxioCam ERc5s Optical microscope was used for microstructural characterization.

Figure 3.5 Zeiss AxioCam ERc5s Optical microscope

3.1.6 Scanning Electron Microscope (SEM)

The scanning electron microscope (SEM) is a type of electron microscope in which focussed electron beams of high energies scans the solid surface and form micrographs. The interaction between the electron beams and the atoms present on the sample surface generate signals that enables us to analyse properties like morphology, composition, electrical conductivity, topography etc. Various kinds of signals can be produced by an SEM ranging from secondary and back-scattered electrons to characteristic x-rays. The high resolution of SEM helps in obtaining images of specimens with varying sizes from those visible to the naked eye to those of nanometric dimensions. [16] The microstructure of the α- Al_2O_3 obtained were characterized using a JEOL JSM-6480LV scanning electron microscope (SEM). [17] The JEOL JSM-6480LV scanning electron microscope was equipped with an INCAPentaFET-x3 X-ray microanalysis system with a high-angle ultra-thin window detector and a 30 mm^2 Si (Li) crystal.

Figure 3.6 JEOL JSM-6480LV Scanning electron microscope

3.1.7 Field-emission scanning electron microscope (FESEM)

A FESEM works with high energy electrons like SEM. These electrons are liberated by a field emission source. The scanning takes place on the surface of the solid sample in a zig-zag pattern. The electron beams generated by a Field Emission Source, when accelerated under vacuum, bombard the sample resulting in emission of different types of electrons from the specimen. A detector detects these signals and produces images on a monitor. This has a much higher resolution and magnification as compared to SEM. A FEI NOVA NANO SEM 450(FEG) field-emission scanning electron microscope (FESEM) was also used for microstructural characterization.

Figure 3.7 FEI NOVA NANO SEM 450(FEG) field-emission scanning electron microscope

3.1.8 Transmission Electron Microscopy (TEM)

Transmission electron microscopy (TEM) is technique in which high energy electron beams(upto 300KV) are transmitted through an ultra-thin specimen. The electrons interact with the specimen as they pass through it. During transmission, the electron beams are scattered. The signals are sensored by a system and then are converted to images which are displayed on the monitor. The resolution of HRTEM is extremely high and it is widely used to confirm the nanometric size of particles .A JEM-2100 JEOL HRTEM with point to point resolution of 0.194 nm was used for analyzing the structure of the alumina.

Figure 3.8 JEM-2100 JEOL HRTEM

3.1.9 Fourier Transform Infrared Spectroscopy (FTIR)

FTIR relies on the fact that most of the molecules absorb light in the infra-red region of the electromagnetic spectrum. FTIR gives the IR spectrum of absorption, emission, scattering et in a wide spectral range of wavelengths. It converts the raw data into actual spectrums. The background emission spectrum of the IR source is first recorded, followed by the emission

spectrum of the IR source with the sample in place. The ratio of the sample spectrum to the background spectrum is directly related to the sample's absorption spectrum. The resultant absorption spectrum from the bond natural vibration frequencies indicates the presence of various chemical bonds and functional groups. In this case, the Spectroscopic analysis was performed in Shimadzu IR Prestige 21 FTIR.

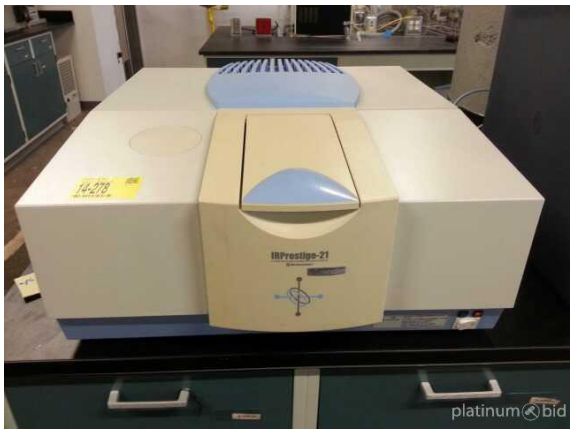

Figure 3.9 Shimadzu IR Prestige 21 FTIR

3.1.10 TG-DSC

Besides, thermal analysis of the powder was also carried out using a differential scanning calorimeter (DSC) to find out the phase transformations that takes place during heating. The dry powder was heated up to 1200^{o}C, with a heating rate of 10^{o}C/minute. Thermogravimetric analysis (TGA) was also performed. The DTA (Differential Thermal Analysis) was carried out by Mettler-Toledo 821.

3.1.11 Vickers Microhardness

The Microhardness testing of metals, ceramics, and composites is useful for a variety of applications for which 'macro' hardness measurements are unsuitable. The Vickers hardness test method consists of indenting the specimen with a pyramid shaped, square based diamond indenter . The specimen can be subjected to a load of 1 to 100 Kgf. The required load is usually applied for 10 to 15 seconds. The lengths of the two diagonals of the indentation on the surface of the material are measured after the load removal and their arithmetic mean is calculated. The area of the indentation surface is also calculated. The Vickers hardness is then obtained by dividing the load by the square mm area of indentation.

F= Load in Kgf

d = Average of the two diagonals, d1 and d2 in mm

HV = Vickers hardness

$$\mathbf{HV = (2FSin136^{o}/2)/d^{2} = 1.854F/d^{2}}$$

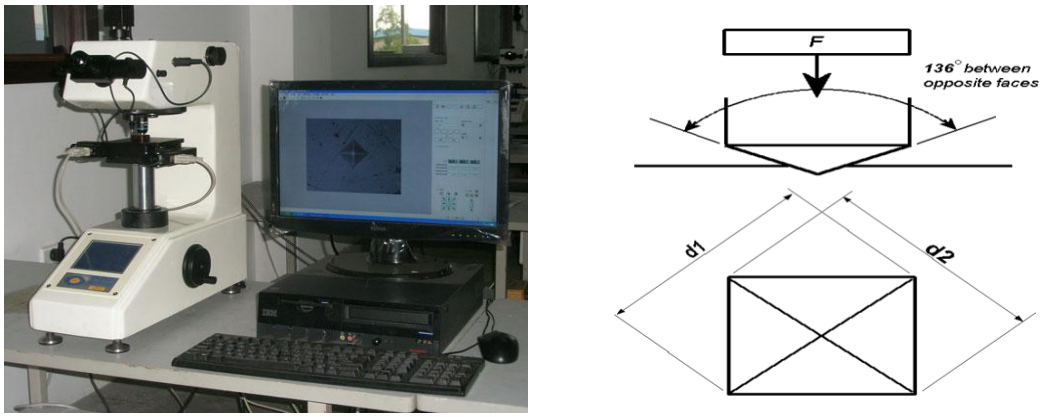

Figure 3.10(a) Vickers Microhardness tester (b) Schematic figure of Vickers pyramid diamond indentation

3.1.12 Ball-on-Plate Wear Tester

The gradual and progressive loss of materials from the body surface in contact with another surface is known as wear. The wear rate of the specimen surface depends on two factors: the tribological conditions to which the surface is subjected, and the response of the material to these conditions. [18] The two major factors in wear are the relative motion between the two contact surfaces and the initial point of contact between the asperities. This test shows the materials' resistance to wear with respect to time. A computerized ball-on-plate wear tester (TR-208-M1, DUCOM) containing a diamond indenter is used in this present research work. 4 mm track was formed on the compact surface when 15 N load is applied for 10 minutes.

Figure 3.11 Ball-on-plate wear tester

3.2 Materials used

- Aluminium chloride ($AlCl_3$)
- Ethanol (C_2H_5OH)
- Ammonia (NH_3)
- Aluminium nitrate ($Al(NO_3)_3$)
- Malic acid ($C_4H_6O_5$)
- Polyvinylpyrrolidone, PVP($(C_6H_9NO)_n$)
- Zinc (Zn) Powder
- Commercially available α-Al_2O_3 powder

3.3 Experimental Procedure

The following work plans have been adopted:

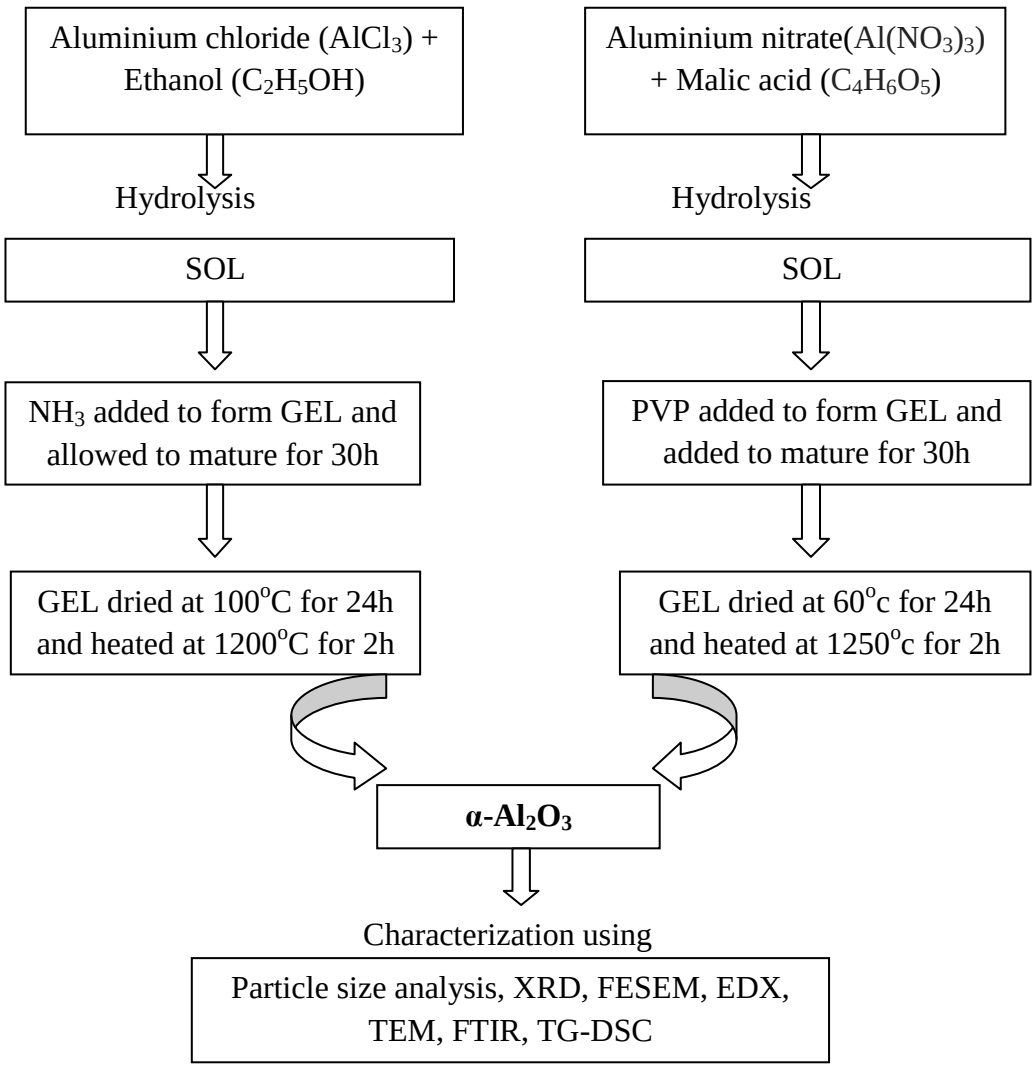

Figure 3.12 Work plan 1 for present investigation

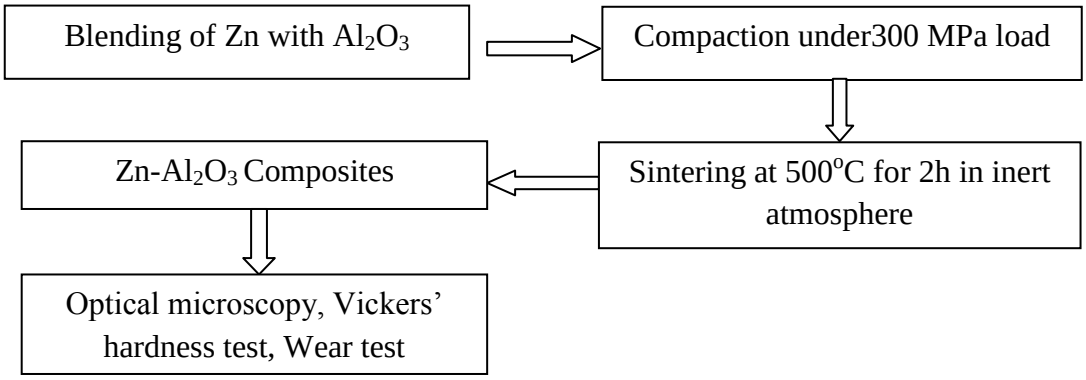

Figure 3.13 Work plan 2 for present investigation

3.3.1 Synthesis of α-Al_2O_3 by Sol-gel Processes

The precursor used for the synthesis of α-Al_2O_3 is aluminium chloride ($AlCl_3$) in an alcoholic medium (ethanol). The other reagent used in the process is NH_3. In this process a 0.1 molar $AlCl_3$ ethanolic solution was prepared by adding ethanol to $AlCl_3$. Magnetic stirring for around 30 minutes was done in order to dissolve $AlCl_3$ in the ethanol. Subsequently around 28% NH_3 solution was added into the mixture under continuous stirring at a consistent feed rate which resulted in formation of a gel. The gel was allowed to mature at room temperature for 30 h. Later the gel was dried at 100°C for 24 h in an oven. [19] Finally the gel was calcined at 1200°C for 2 h in a furnace. [20] The calcined sample was then milled in a planetary ball mill for 30 h to further reduce the crystallite size range.

Reactions:

$$AlCl_3 + C_2H_5OH \rightarrow Al(O\,C_2H_5)_3 + HCl \quad \ldots(1)$$

$$Al(O\,C_2H_5)_3 + H_2O \rightarrow C_2H_5OH + Al(OH)_3 \quad \ldots(2)$$

$$2Al(OH)_3 \rightarrow AlO(OH) \rightarrow \gamma\text{-}Al_2O_3 + \alpha\text{-}Al_2O_3 \rightarrow \alpha\ Al_2O_3 \quad \ldots(3)$$

α-Al_2O_3 was also synthesized by another route. The precursor materials for the synthesis of alumina by the second method are aluminium nitrate, malic acid and polyvinylpyrrolidone(PVP). In this process the precursor sol was prepared by sol-gel technique using aluminium nitrate and malic acid. The gel was synthesized by mixing aluminium nitrate, malic acid and PVP in the mass ratio of 10:3:1.5. The gel was heated at 60°C for 24 h in an oven. The alumina synthesized was heat treated at 1250°C for 2 h. The resultant was found to be α- Al_2O_3. [21]

Reactions: $3C_4H_6O_5+2Al(NO_3)_3 \rightarrow Al_2(C_4H_4O_5)_3+6HNO_3$ …(4)

$Al_2(C_4H_4O_5)_3+6H_2O \rightarrow 2Al(OH)_3+3C_4H_6O_5$ ...(5)

$2Al(OH)_3 \rightarrow AlO(OH) \rightarrow \gamma\text{-}Al_2O_3 + \alpha\text{-}Al_2O_3 \rightarrow \alpha\ Al_2O_3$ ...(6)

3.3.2 Characterization of α-Al_2O_3

The alumina synthesized by the sol-gel process were analysed by particle size analysis and XRD to characterize the powders in terms of their crystallinity and crystallite size. Microstructural characterization and analysis were performed using field emission scanning electron microscopy (FESEM) and transmission electron microscope (TEM).The further characterizations of particles were carried out by EDX, TG- DSC and FTIR techniques.

3.3.3 Ex-situ Synthesis of Zn-α-Al_2O_3 Composites

Commercially available elemental Zinc (Zn) has been blended with α-Al_2O_3 to produce Zn-50 vol. % Al_2O_3 and Zn-60 vol. % Al_2O_3 powders which are compacted under a load of approximately 300 MPa in a hydraulic press machine and are subjected to heat treatment (sintering) at 500°C for 2h to give rise to hard and dense compacts of Zn-Al_2O_3 composites.

3.3.4 Characterization of Zn-Al_2O_3 Composites

The microstructures of the green compacts as well as sintered compacts of the MMC obtained were characterized using optical microscopy. Apart from these mechanical properties were tested by wear and hardness tests.

CHAPTER-4

RESULTS AND DISCUSSIONS

4.1 Characterization of the α-Al_2O_3 developed by Sol-gel process

α-Al_2O_3 particles are synthesized using $AlCl_3$ and $Al(NO_3)_3$ as precursors by the sol-gel process. The alumina particles formed from $AlCl_3$ were milled by ball milling for a period of 30 h in a planetary ball mill in order to further decrease its particle size. The alumina thus synthesized by the two processes were analyzed using various characterization techniques like particle size analysis, x-ray diffraction (XRD), field emission scanning electron microscopy (FESEM), transmission electron microscopy (TEM), differential thermal analysis (DTA) etc. The results and the interpretations of their analysis methods are as follows:

4.1.1 Particle size analysis of Alumina

Figure 4.1(a) shows the particle size distribution of α-Al_2O_3 powder synthesized using $AlCl_3$ as precursor and it was observed that the average diameter of the Al_2O_3 particles was around 5.57 µm. The particle size distribution suggests that there is a significant vol. % of particles less than the average as well as above the average particle size. The particle size distribution of Al_2O_3 synthesized using $Al(NO_3)_3$ as precursor is shown in Figure 4.1(b). It was observed that this alumina has a much smaller particle size as compared to Al_2O_3 synthesized using $AlCl_3$ as precursor and the particle size distribution is Gaussian with average size of the particle as 0.74 µm.

(a)

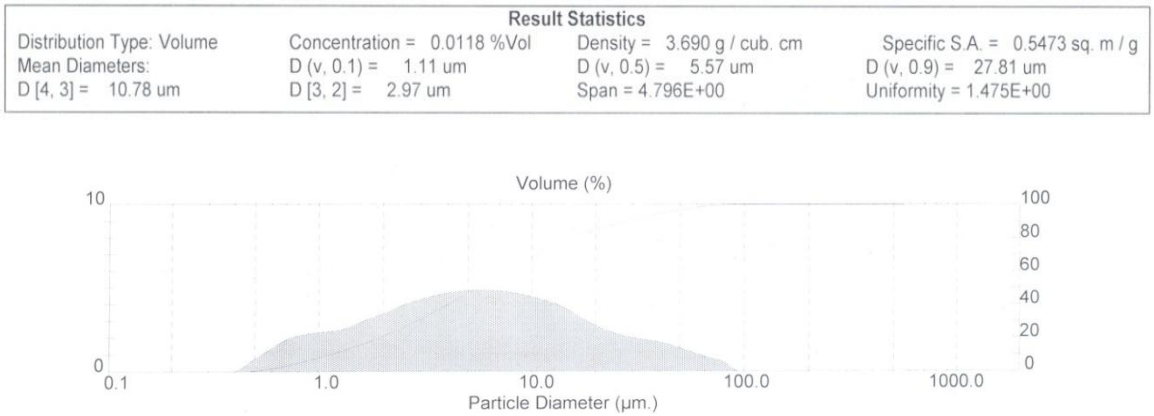

(b)

		Size (r.nm):	% Intensity	Width (r.nm):
Z-Average (r.nm): 741.8	Peak 1:	115.5	100.0	8.057
PdI: 1.000	Peak 2:	0.000	0.0	0.000
Intercept: 1.27	Peak 3:	0.000	0.0	0.000

Result quality : Refer to quality report

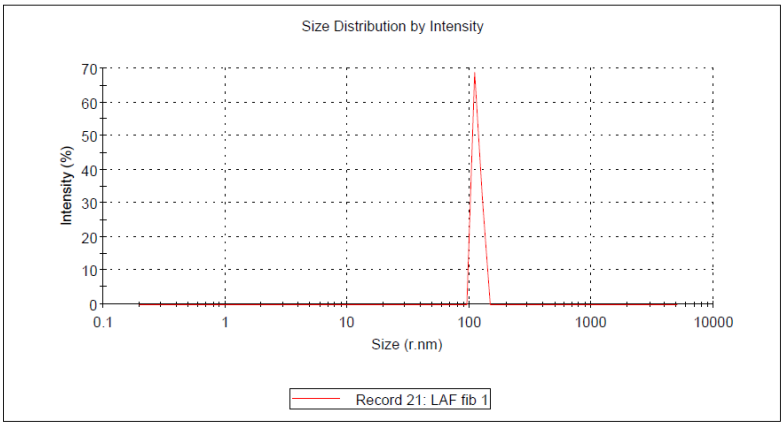

Figure 4.1 Particle size distribution of α-Al_2O_3 powder synthesized using (a) $AlCl_3$ (b) $Al(NO_3)$ as precursor

4.1.2 XRD analysis

Figure 4.2(a, b) show x-ray diffraction images for the powders obtained from different precursors, $AlCl_3$ and $Al(NO_3)_3$, dried and heat treated for 2 h at temperatures 1200^oC and 1250^oC respectively. The alumina synthesized by both the processes show identical peak positions in the x-ray diffraction plots. When $AlCl_3$ was used as a precursor, the dried gel contains mainly $AlCl_3 \cdot 6H_2O$. Thermal treatment of the gel leads to decomposition of $AlCl_3 \cdot 6H_2O$ and results in the formation of a mixture of γ-Al_2O_3 and α-Al_2O_3. The dried mass when heat treated to 1200^oC for 2 h results in the formation of only α-Al_2O_3. 30 h milling of the α-Al_2O_3 obtained using $AlCl_3$ as the precursor after calcining at 1200^oC for 2 h has led to considerable broadening of the peaks as can be seen in Fig. 4.2(a).

The crystallite size was determined from the x-ray diffraction data using the Scherer equation. The crystallite size of α-Al_2O_3 obtained using $AlCl_3$ as the precursor after calcining at 1200^oC for 2 was found to be 199 nm. This α-Al_2O_3 after 30 h of milling was found to have a crystallite size of 26 nm. The mean crystallite size of the alumina produced using $Al(NO_3)_3$ as precursor was found to be 114 nm.

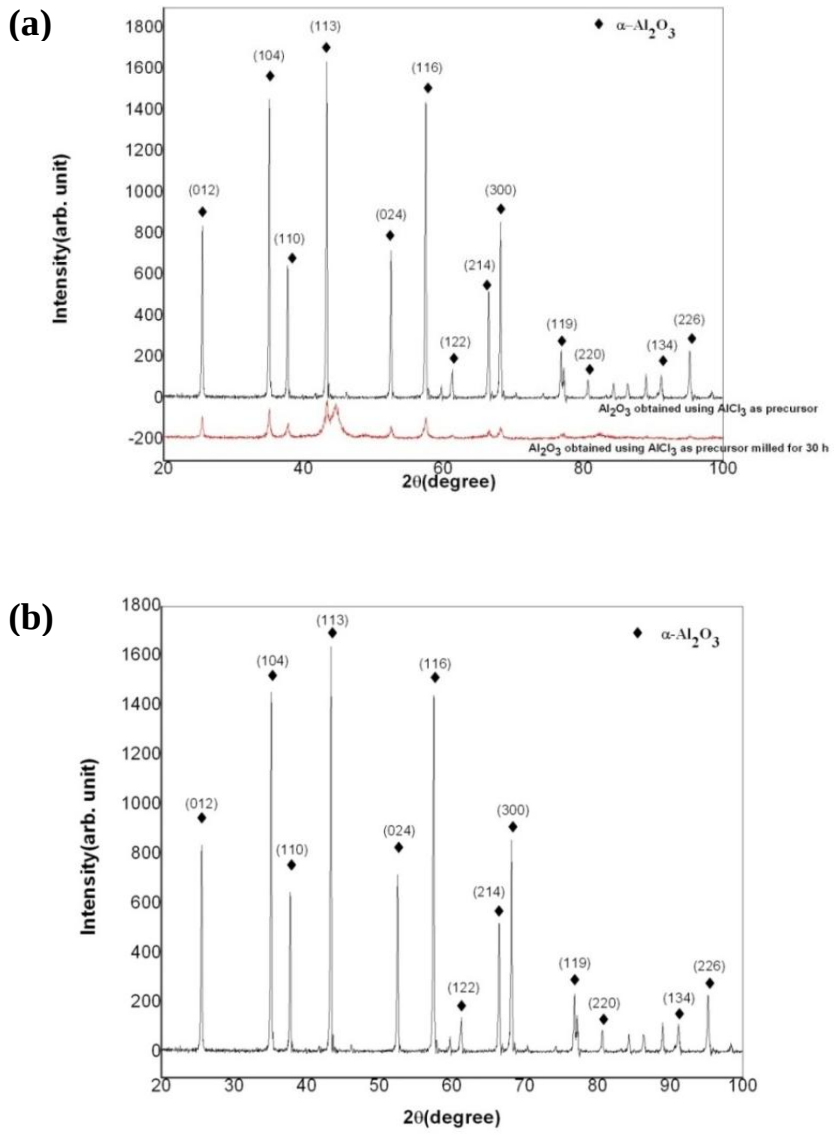

Figure 4.2(a) XRD plot of α-Al_2O_3 powder synthesized using $AlCl_3$ and α-Al_2O_3 obtained after milling for 30 h (b) XRD plot of α- Al_2O_3 powder synthesized using $Al(NO_3)_3$ as precursor

4.1.3 FESEM-EDX

The FESEM images of the Al_2O_3 sample obtained from $AlCl_3$ as precursor after calcining at 1200^{o}C for 2 h is shown by Figure 4.3 (a,b). The images show the presence of agglomerates of different geometries. The EDX analysis of the 30 h milled powder in Figure 4.3(c) shows that the atomic % of Al is 37.61 and the atomic % of O is 62.39 in the Al_2O_3 sample obtained from $AlCl_3$ as precursor. The EDX analysis of the 30 h milled powder suggests that the composition of the powder is very close to the stoichiometric composition of Al_2O_3. Figure 4.4 (a,b) show the FESEM images of α-Al_2O_3 powder obtained from $Al(NO_3)_3$ as precursor.

The alumina synthesized by using $Al(NO_3)_3$ as precursor was found to be fibrous and hence has a higher aspect ratio as compared to the alumina synthesized from $AlCl_3$. FSEM images suggest that they are plate like instead of particles which were seen in the case of alumina synthesized using $AlCl_3$ as precursor. With the increase in aspect ratio, various properties of the material improves thereby leading to a unique combination of excellent mechanical, electrical and magnetic properties as well making them an ideal reinforcing agent for high strength composites. Figure 4.4(c) shows the EDX analysis of α-Al_2O_3 powder synthesized using $Al(NO_3)_3$ as precursor. The EDX analysis suggests that the Al_2O_3 is highly stoichiometric where the atomic % of Al is 40.4 and the atomic % of O is 59.6.

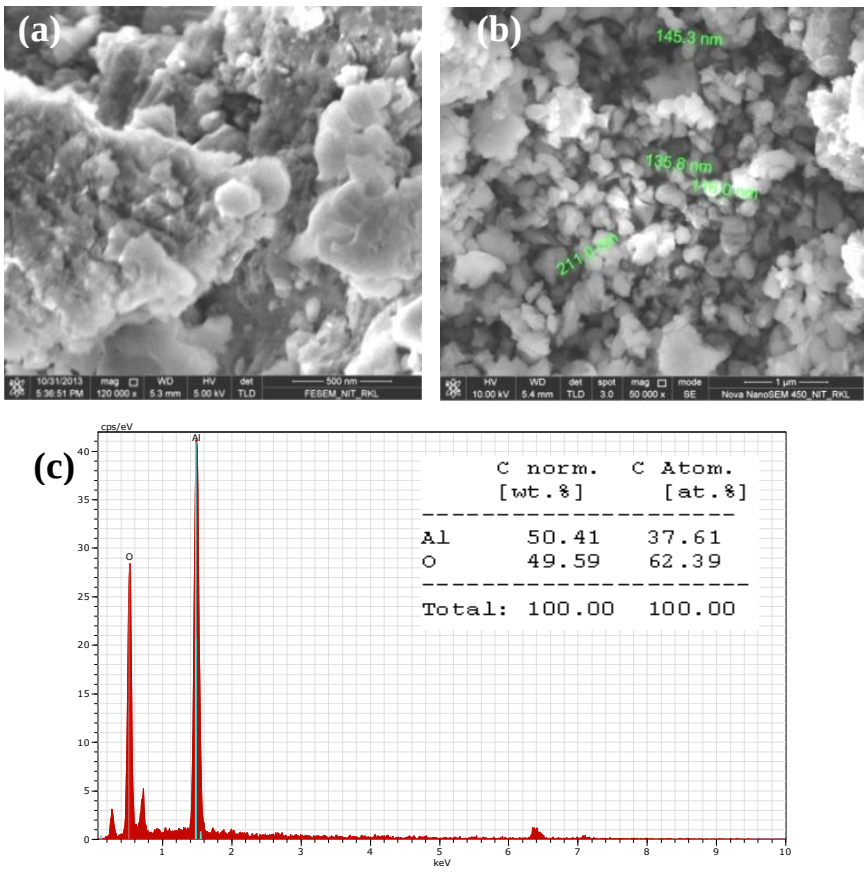

Figure 4.3(a, b) FESEM images of α-Al_2O_3 powder obtained from $AlCl_3$ as precursor after calcining at 1200^{o}C for 2 h (c) EDX of α-Al_2O_3 powder obtained from $AlCl_3$ as precursor

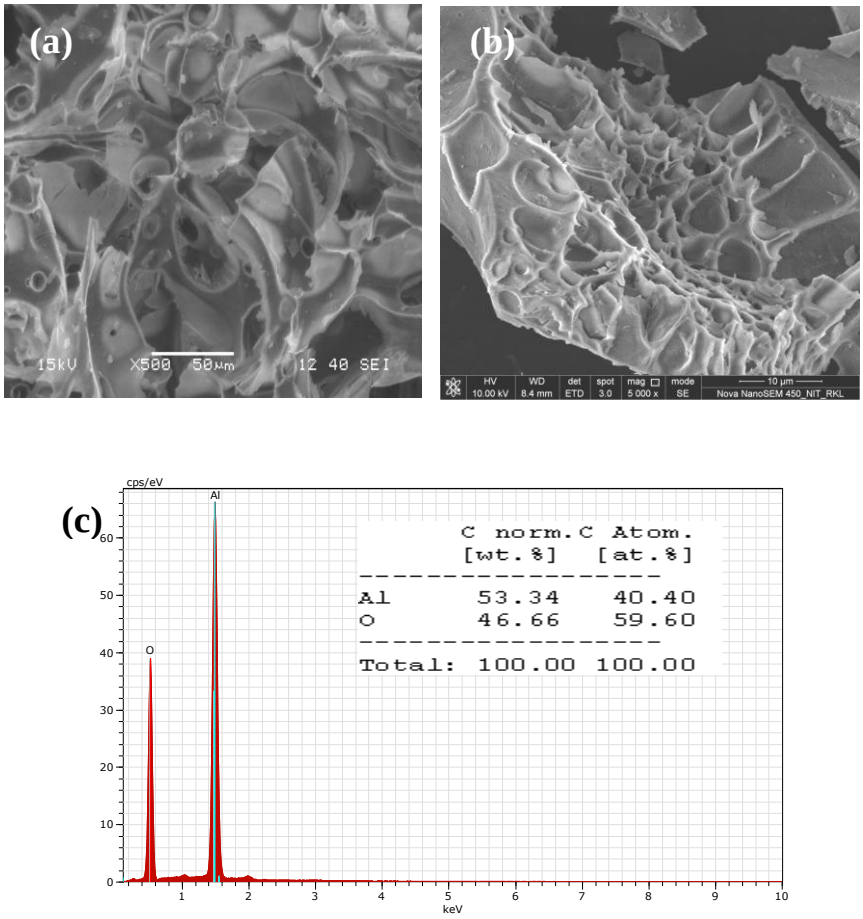

Figure 4.4 (a, b) FESEM of α- Al_2O_3 powder obtained from $Al(NO_3)_3$ as precursor (c) EDX of α- Al_2O_3 powder obtained from $Al(NO_3)_3$ as precursor

4.1.4 TEM

The TEM analysis was carried out in order to find out the particle size of alumina powders obtained by the sol-gel method using different precursors. The TEM images of α-Al_2O_3 powder in Figure 4.5(a) obtained from $AlCl_3$ as precursor milled for 30 h confirms that the alumina crystallites were nanometric in dimension. The spot pattern seen in the SAED (selected area electron diffraction) image in Figure 4(b) suggests the high degree of crystallinity of the alumina particles. Figure 4.6(a) shows the TEM micrograph of α-Al_2O_3 powder obtained from $Al(NO_3)_3$ as precursor. The spot patterns in the SAED image in Figure 4.6(b) confirm the high degree of crystallinity of this α-Al_2O_3.

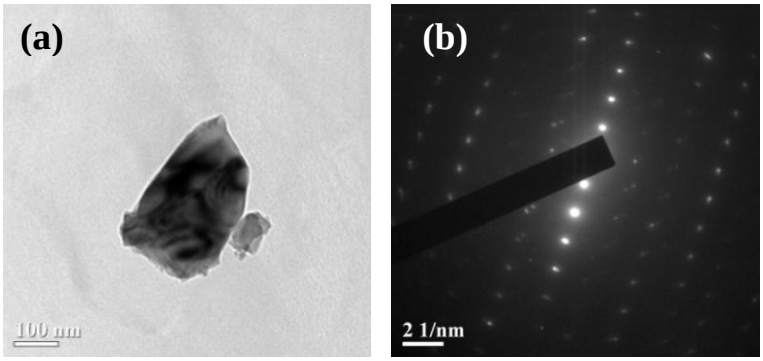

Figure 4.5(a) TEM of α-Al_2O_3 powder obtained from $AlCl_3$ as precursor and milled for 30h (b) Spot pattern obtained from the SAED (Selected area electron diffraction) image of this alumina

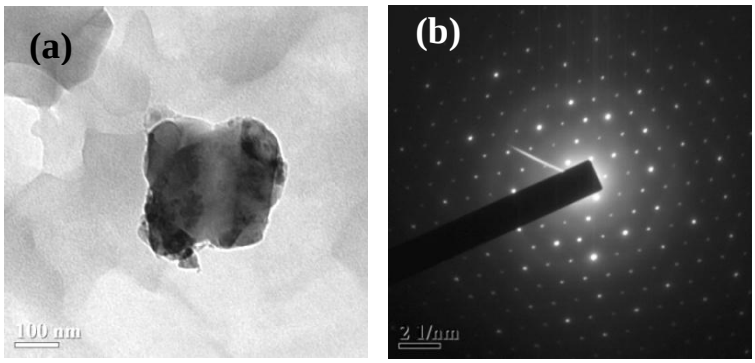

Figure 4.6(a) TEM of α- Al_2O_3 powder obtained from $Al(NO_3)_3$ as precursor (b) Spot pattern obtained from the SAED (Selected area electron diffraction) image of this alumina

4.1.5 FTIR

The Figure 4.7 (a) shows the FTIR spectra of α-alumina synthesized from $AlCl_3$ as precursor. The IR absorption bands observed in the range 1600-1650 cm^{-1} and 3000-3700 cm^{-1} could be assigned to the O-H vibration mode. These bands are assigned to the bending vibration and stretching vibration of the O-H bond due to the absorbed water. Figure 4.7(a) shows a broad O-H stretching band at around 3400 cm^{-1} which corresponds to O-H stretching of Al_2O_3 surface. The positions of the peaks associated to the -OH group of alumina at 2090 cm^{-1} can be used as fingerprints of the bohemite structure (AlOOH). The broad absorption peaks exhibited by this solid indicates the formation of an amorphous hydrated alumina. The bands around 450^{-1} cm and 525^{-1} cm are due to the Al-O stretching. The absorption bands at around 950 cm^{-1} possibly correspond to the bending of Al-OH group. The peaks at 2950 and 2860 cm^{-1} are possibly due to C-H aliphatic stretch. The C-H bonds are possibly from the ethanol used during the synthesis of Al_2O_3 from $AlCl_3$ as precursor. The band at 1360 cm^{-1} is due to the C-O stretching mode. The IR absorption band at 2250 cm^{-1} is possibly due to the -C≡N

stretching. These bonds have been possibly formed due to the reaction of ethanol and NH_3. It has been reported that the -C≡N stretching bands of most of the nitriles are in the range of 2300-2200 cm^{-1}. The broad absorption in the 950-1200 cm^{-1} range, indicates the formation of Al-O-Al bonds. Bands due to alumina are present at 1400, 1034 and 563 cm^{-1}.

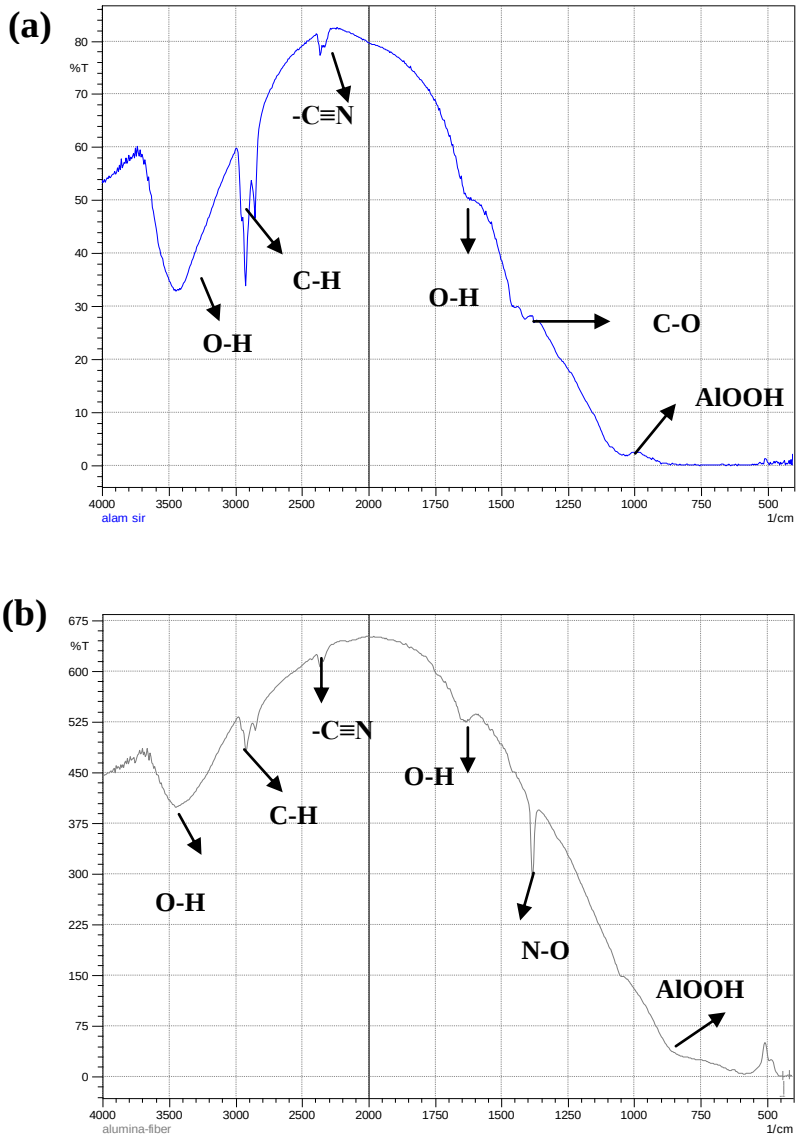

Figure 4.7 (a) FTIR spectra of α-Al_2O_3 from $AlCl_3$ as precursor after calcining at 1200°C for 2h (b) FTIR spectra of α-Al_2O_3 from $Al(NO_3)_3$ as precursor after calcining at 1250°C for 2 h

Figure 4.7(b) shows the FTIR spectra of α-alumina synthesized from $Al(NO_3)_3$ as precursor after calcining at 1250°C for 2 h. This process of synthesis has led to α-Al_2O_3 having crystallite size smaller than the previous technique. The α- Al_2O_3 synthesized had crystallite size of 114 nm as compared to the crystallite size of α-Al_2O_3 obtained by the previous method where the crystallite size was found to be 199 nm. Smaller particles which have size

similar to that of the wavelength of the light waves interact with the light waves and therefore lead to a broader peaks and slanted baselines. This is the reason why we see much broader peaks in this case. The broadening is due to the reduction in crystallite size. Broader peaks indicate increase in interaction with the light wave. There is no considerable change in transmission peak positions. The broad IR peak at around 3400 cm^{-1} is due to the O-H group. The absorption band observed around 1650 cm^{-1} could also be assigned to the OH vibrational mode possibly due to the moisture absorbed in the sample. The peaks at 2950 and 2860 cm^{-1} is possibly due to C-H aliphatic stretch. The peak between 1350-1400 cm^{-1} is possibly due to the N-O group which possibly came from the precursor $Al(NO_3)_3.9H2O$. Reaction of the precursor materials also lead to the formation of HNO_3 which later decomposes to give NO_3. Both the FTIR analysis in Figures 4.7(a, b) for α-Al_2O_3 synthesized from $AlCl_3$ and from $Al(NO_3)_3$ as precursor respectively show similar peaks but the FTIR spectra of α- Al_2O_3 obtained from $Al(NO_3)_3$ as precursor after calcining at 1250^{o}C for 2 h shows a strong peak due to N-O group.

4.1.6 TG-DSC

The TG-DSC result for 30h milled α-Al_2O_3 powder obtained by sol-gel method from $AlCl_3$ is shown in Figure 4.8 (a). It was observed that up to the temperature of 220^{o}C there is a weight gain of around 0.73%. In the region between 220 to 700^{o}C there is a total weight gain of 13.11%. Weight loss of the material is less than 0.19 % which takes place between 800 to 1200^{o}C. In this region we also see a lot of fluctuation in temperature. An endothermal peak at 440.9^{o}C is observed which can be attributed to the pseudomophic phase transformation of bohemite (γ-Al(O)OH) to γ- Al_2O_3. It should be noted that during thermal treatment, stable α-Al_2O_3 phase is obtained through the following phase transformations:

$$\text{hydrous alumina} \rightarrow \text{bohemite } (\gamma\text{-Al(O)OH}) \rightarrow \gamma \rightarrow \delta \rightarrow \theta \rightarrow \alpha$$

The weight gain of the sample takes place simultaneously with the endothermic reaction. Figure 4.8 (b) shows the thermal analysis of α- Al_2O_3 powder obtained by sol-gel method from $Al(NO_3)_3$ as precursor where it is calcined at 1250^{o}C for 2h. Here we do not see any exothermic or endothermic reaction taking place as the temperature is raise form room temperature to 1200^{o}C. The plot shows that there is a slight loss in weight of the sample due to evaporation of adsorbed water. Weight loss of the charged material is found to be less than 1%. There is no sign of exothermic or endothermic reaction in the sample.

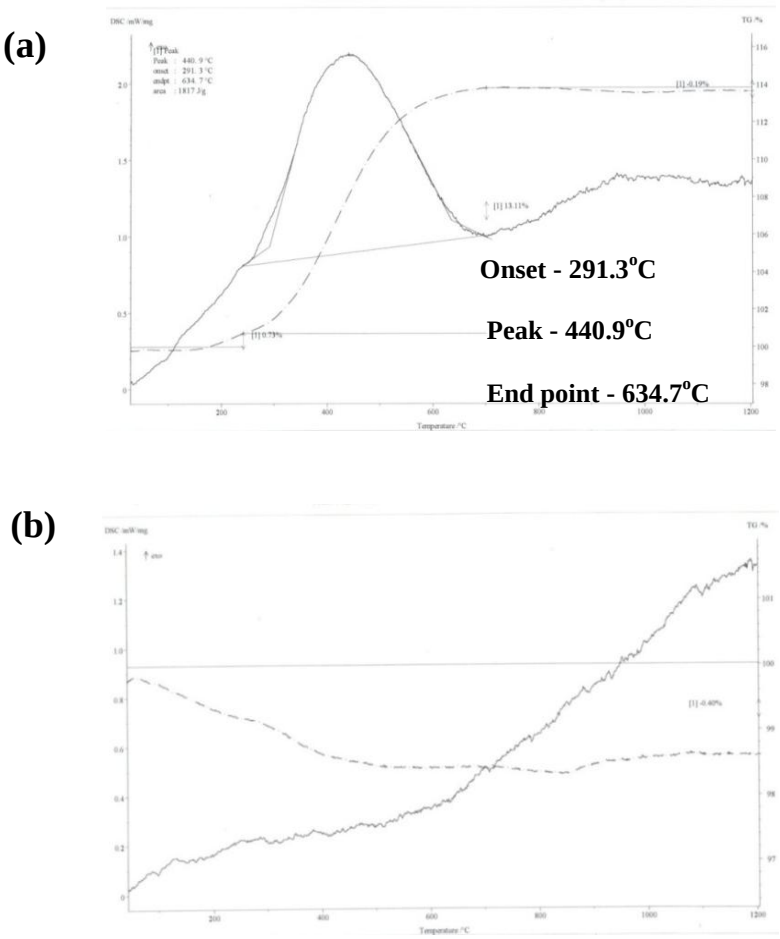

Figure 4.8 (a) Thermal analysis of milled α- Al_2O_3 powder obtained by sol-gel method from $AlCl_3$ (b) Thermal analysis of α- Al_2O_3 powder obtained by sol-gel method from $Al(NO_3)_3$

4.2 Characterization of Zn-Al_2O_3 Composites

Zn-50 vol. % and Zn- 60 vol. % α-Al_2O_3 composites were developed by powder metallurgy route. The Zn and Al_2O_3 powders were mixed in required proportions and were compacted under a load of 300 MPa followed by sintering at 500°C for 2 h in argon gas atmosphere. The melting point of Zn is 419.53°C which is lower than the sintering temperature; hence it is a liquid phase sintering process. The green as well as sintered compacts were observed using optical microscopy. Besides this, the mechanical properties of the composites were characterized by Vickers hardness and ball-on-plate wear tester.

4.2.1 Optical microscopy

Figure 4.9(a, b) show the optical micrographs of green and sintered compacts of pure Zn respectively. The green compact was sintered at 500°C for 2 h in Argon atmosphere in a tubular furnace. Both the figures show a single light coloured phase of pure metallic Zn.

Figure 4.9(b) shows less porosity and more uniform surface as a result of sintering at 500^{o}C. Figure 4.10(a, b) depicts the optical micrographs of green and sintered samples of Zn-50 vol. % Al_2O_3 respectively. Both the figures clearly depict two distinct phases, one light coloured phase corresponding to metallic Zn and a darker phase corresponding to Al_2O_3. Liquid phase sintering takes place at the sintering temperature of 500^{o}C since Zn has a melting point of 419.5^{o}C. As Zn (ρ = 7.14 gm/cc) has a higher density compared to Al_2O_3 (ρ = 3.95 gm/cc) it is possible that Al_2O_3 floats in molten Zn whereas Zn remains at the bottom during sintering. Figure 4.11(a, b) show the optical micrographs of green and sintered samples of Zn-60 vol. % Al_2O_3 respectively. The green compacts in all the three cases were not polished, hence they appear darker and the phases are not distinctly visible. Figure 4.11(b) shows that the Zn-60 vol. % Al_2O_3 composite like the Zn-50 vol. % Al_2O_3 composite shows distinct light and dark phases corresponding to metallic Zn and Al_2O_3 respectively. However the fraction of Al_2O_3 is higher in the case of Zn-60 vol. % Al_2O_3 composite which is indicated by the presence of larger fraction of dark areas.

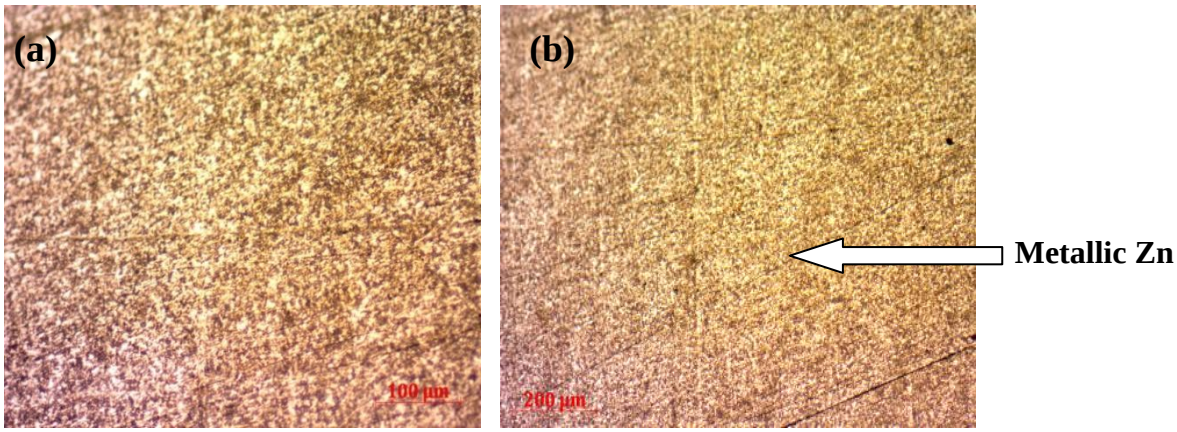

Figure 4.9 Optical micrographs of (a) green and (b) sintered compacts of pure Zn respectively

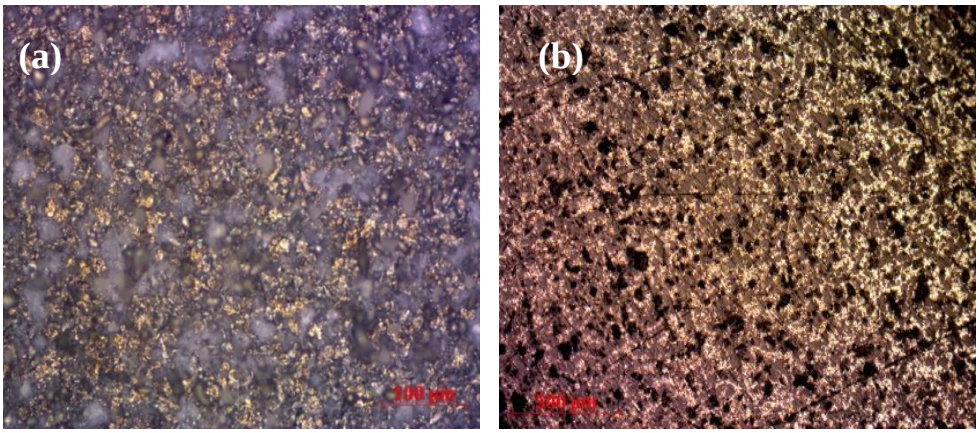

Figure 4.10 Optical micrographs of (a) green and (b) sintered compacts of Zn-50 vol. % Al_2O_3 respectively

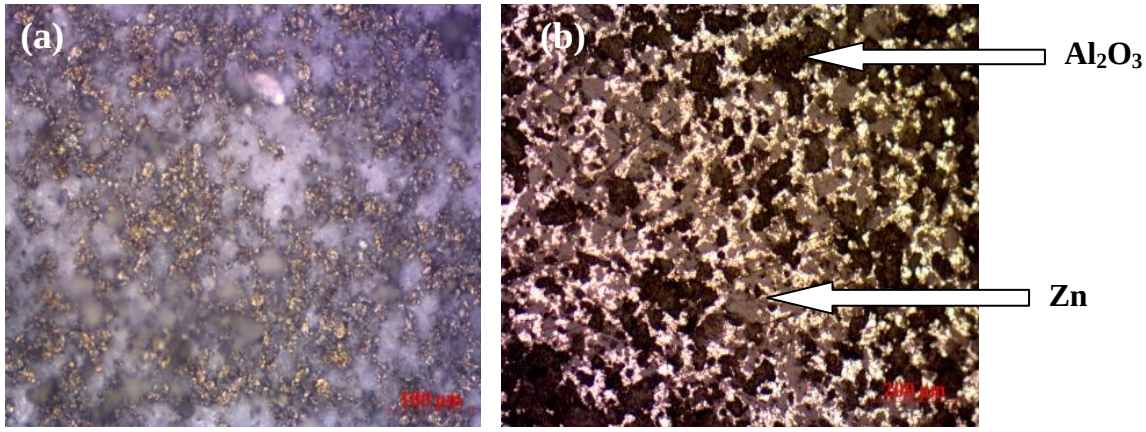

Figure 4.11 Optical micrographs of (a) green and (b) sintered compacts of Zn-60 vol. % Al_2O_3 respectively

4.2.2 Vickers Hardness Test

The Vickers hardness test was carried out by using a load of 5 Kgf. Table 4.1 lists the hardness values of sintered Zn and the various Zn-Al_2O_3 composites. The result of the hardness test indicates that the hardness of Zn-60 vol. % Al_2O_3 sample sintered at 500^{o}C for 2 h is higher as compared to the hardness of pure Zn samples sintered at the same temperature. Figure 4.12 shows the variation of hardness in both pure Zn and Zn-50, 60 vol. % Al_2O_3 composites. The plot clearly suggests that the Al_2O_3 reinforcement in the soft Zn matrix results in significant improvement of hardness in the Zn-Al_2O_3 composites. The hardness of the Zn-Al_2O_3 composites increase with the increase in the vol. % of Al_2O_3 in the composites. Zn has a density of 7.14 gm/cc and the density of Al_2O_3 is 3.95 gm/cc. As Al_2O_3 is lighter as compared to Zn so it is expected to remain at the surface of the sample during liquid phase sintering. Due to the better mechanical properties of Al_2O_3 the hardness at surface of the compact would be better as compared to the inside of the compact.

Table 4.1 Hardness values of sintered Zn and Zn-Al_2O_3 composites

Sample (sintered at 500^{o}C for 2 h)	**Hardness (MPa)**
Zn	440.6
Zn- 50 vol. % Al_2O_3	550.8
Zn-60 vol.% Al_2O_3	590.3

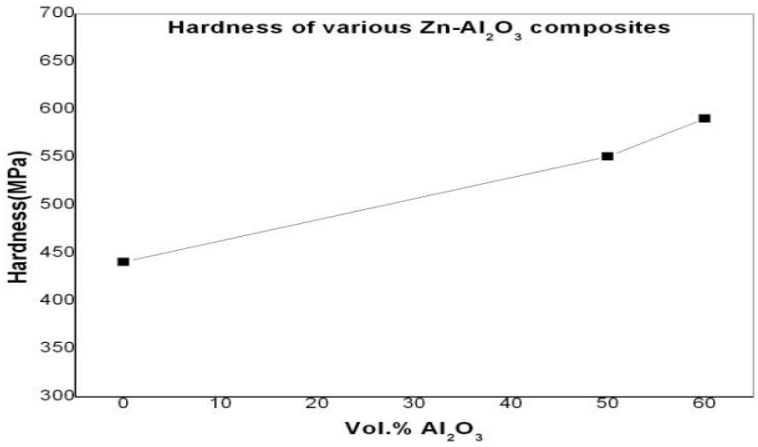

Figure 4.12 Variation of hardness in pure Zn and Zn-50, 60 vol. % Al_2O_3 composites

4.2.3 Wear Test

A ball-on-plate wear tester was used to carry out the wear test. The wear studies have been done under a load of 15 N for a period of 10 minutes at a rotational speed of 15 rpm. The track diameter was 4 mm. The plot in Figure 4.13 shows the variation of wear depth with respect to time for pure Zn and Zn-50, 60 vol. % Al_2O_3 composites. This plot shows clearly that the wear depth goes on increasing with the increase in time. In the case of Zn-Al_2O_3 composites sintered at 500^{o}C for 2 h there is a slightly lower mass loss during the wear test as compared to the pure Zn sintered sample. The wear resistance of the Zn-Al_2O_3 composites increases with the increase in the vol. % of Al_2O_3 in the Zn matrix. This suggests that the Al_2O_3 particles used as reinforcement in the Zn matrix was effective in improving the wear resistance of the Zn-Al_2O_3 composites.

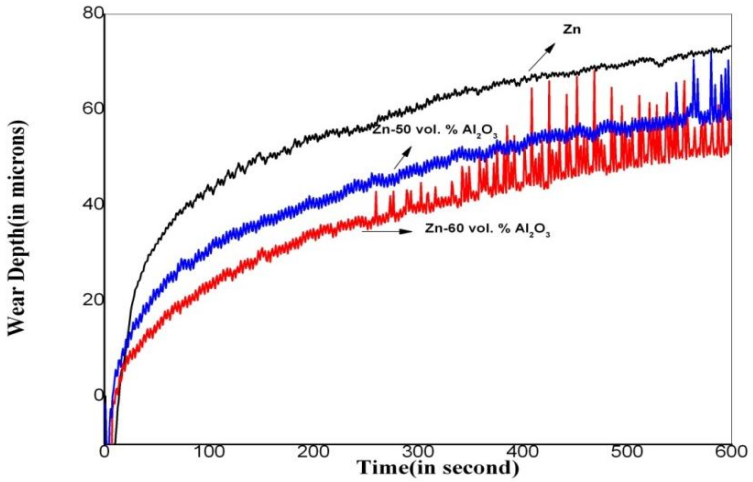

Figure 4.13 Variation of wear depth with respect to time for pure Zn and Zn-50, 60 vol. % Al_2O_3 composite

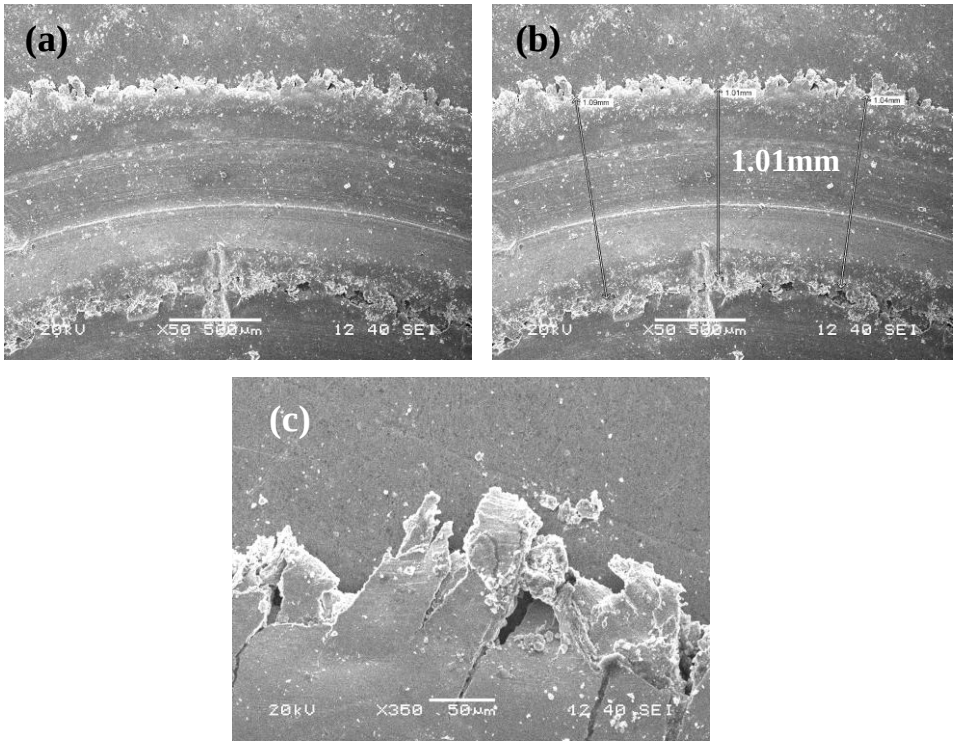

Figure 4.14 (a-c) SEM images of the wear track of pure Zn sintered at 500^{o}C for 2 h

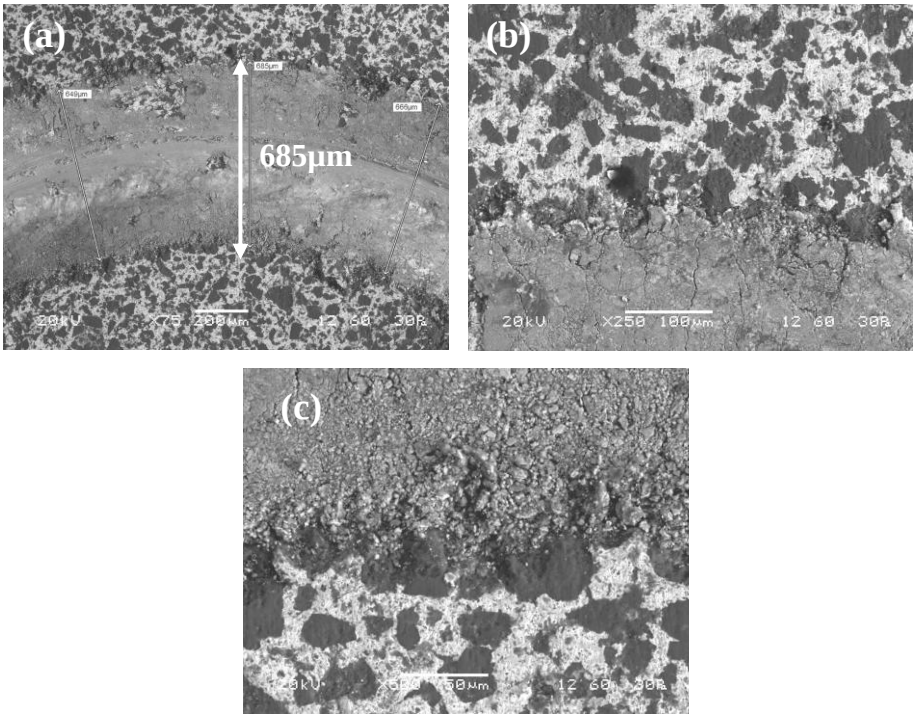

Figure 4.15 (a-c) SEM images of the wear track of Zn-50 vol. % Al_2O_3 sintered at 500^{o}C for 2 h

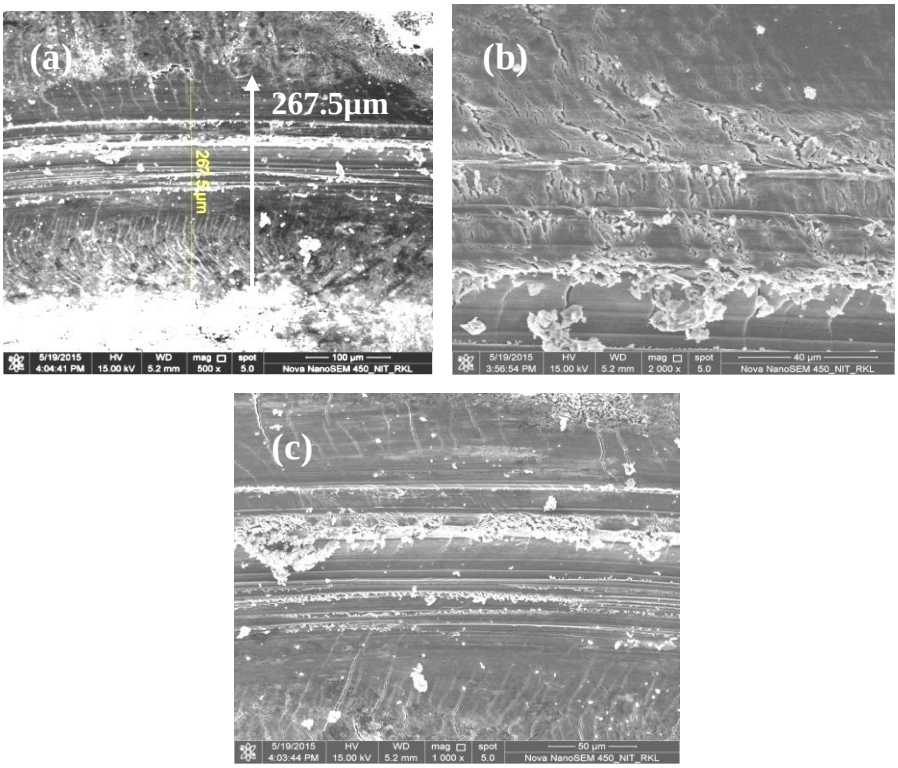

Figure 4.16 (a-c) SEM images of the wear track of Zn-60 vol. % Al_2O_3 sintered at 500^oC for 2 h

Cracks were observed at the wear track in all the three cases. The decrease in wear depth from 1.01mm to 267.5µm suggests that reinforcement of Al_2O_3 in Zn is effective in improving the wear resistance of the Zn-Al_2O_3 composites. White coloured Al_2O_3 particles could be seen in the wear track of Zn-Al_2O_3 samples. Since Al_2O_3 has a higher melting point and a lower density, it gets loosely bonded with Zn at the surface. The wear debris consisted mainly of the Al_2O_3 particles.

CHAPTER-5

CONCLUSIONS

The conclusions that can be drawn from the present research work are as follows:

- α-Al_2O_3 powders of nanometric size were successfully synthesized by sol-gel method using two different precursors, aluminium chloride and aluminium nitrate respectively.
- Characterization of the resultant alumina powders was done by X-ray diffraction, scanning electron microscopy (SEM), field emission scanning electron microscopy (FESEM), transmission electron microscopy (TEM), differential thermal analysis (DTA) and fourier transform infrared spectroscopy (FTIR)
- The high temperatures used for heat treatment resulted in the formation of single phase α- Al_2O_3. It was observed that the crystallite size of alumina decreased from 199nm by using $AlCl_3$ to 114nm by using $Al(NO_3)_3$
- α- Al_2O_3 fibers were formed in the second process.
- The decrease in size accompanied by an increase in aspect ratio makes it an ideal reinforcing agent for high strength composites and results in its highly superior properties
- Addition of Al_2O_3 increased the hardness of the Zn-Al_2O_3 composites.
- The increase in vol. % of Al_2O_3 resulted in an increase in wear resistance of the Zn-Al_2O_3 composites.
- Zn has a density of 7.14 gm/cc and the density of Al_2O_3 is 3.95 gm/cc. As Al_2O_3 is lighter as compared to Zn so it is expected to remain at the surface of the sample during liquid phase sintering. As the mechanical properties of Al_2O_3 are better as compared to that of Zn, the hardness and wear resistance of the Zn-Al_2O_3 composites would be better at the surface of the compact as compared to the inside of the compacts.

SCOPE OF FUTURE WORK

There exists a wide scope of future work in view of the present investigation. The future investigations can be focused on the study of variation of the volume percent of alumina in the zinc matrix and the effect of the different compositions with respect to the mechanical properties. The matrix can be changed and the effect of alumina as a reinforcing agent in various matrices can be studied.

Further investigation can be done to evaluate of efficiency of different methods to improve the properties of composites such as - different types of fabrication methods and addition of different types of nano-fillers in the matrix in different volume fractions. The effect of varying volume fraction of reinforcements and nano-fillers can be investigated.

REFERENCES

1. Colvin V.L., The potential environmental impact of engineered nanomaterials, Nature Biotechnology, vol. 21(2003) , 1166 – 1170
2. Buzea C., Pacheco I. , Robbie K., Nanomaterials and nanoparticles: Sources and toxicity, Biointerphases 2, MR17 (2007)
3. Schwartz M., Encyclopaedia and Handbook of Materials Parts and Finishes. Boca Raton: CRC Press, 2002
4. Eskandari A., Aminzare M., Razavi Hesabi Z., Aboutalebi S.H., Sadrnezhaad S.K., Effect of high energy ball milling on compressibility and sintering behaviour of alumina nanoparticles , Ceramics International, 38 (2012) ,2627–2632
5. Hou Y., Soleimanpour A.M., Jayatissa A.H., Low resistive aluminium doped nanocrystalline zinc oxide for reducing gas sensor application via sol– gel process, Sensors and Actuators B: Chemical, 177(2013) ,761-769
6. Ianăşi C., Mitigation Techniques Of Transverse Displacement Of The Wood Beams, Annals of 'Constantin Brancusi' University of Targu-Jiu Engineering Series , 4(2013), 122
7. Parvin N., Rahimian M., The Characteristics of Alumina particle reinforced pure Al Matrix Composite, Acta Physica Polonica, 121(2012), 108-110
8. Chawla K.K., Composite Material Science and Engineering. New York , Springer-verlag , 1999
9. Harris B., Engineering composite materials. London, IOM, 1999
10. Matthews F.L., Rawlings R.D., Composite Materials: Engineering and Science, Elsevier, London,1999
11. Josmin J., Kuruvilla J., Advances in Polymer Composites: Macro- and Microcomposites - State of the Art, New Challenges, and Opportunities VOL1, Wiley-VCH Verlag GmbH & Co., 2012
12. Kaw A.K., Introduction to Composite Materials (Mechanical Engineering Series), CRC Press, 2005
13. Makvandi R., Öchsner A., On a Finite Element Approach to Predict the Thermal Conductivity of Carbon Fiber Reinforced Composite Materials, Defect and Diffusion Forum, vol 354(2014) , 215-225
14. Randall M., Sintering Theory and Practice, Wiley-VCH ,Germany , January 1996.
15. Coble R.L., Sintering Crystalline Solids: Intermediate and Final State Diffusion Models , Journal Of Applied Physics, 32(1961), 787

16. Ahmed S., Ahsan Q., Kurny A., Effect of rolling on tensile flow and fracture of Al-4.5Cu 3.4Fe cast composite, Journal of Materials Processing Tech., 182 (2007), 215-219
17. Yoshikawa N., Watanabe Y., Mechanical properties of Al-Al_2O_3 composites fabricated by reaction between SiO2 and molten Al, Al-Cu, Journal Of Materials Science Letters, 16 (1997) ,1540-1550
18. Chu J., Nanostructures and sensing properties of ZnO prepared using normal and oblique angle deposition techniques, Thin Solid Films, 520(2012), 3493-3498
19. Hutchings M., Abrasive and erosive wear tests for thin coatings: a unified approach, Tribology International , 31(1998) , 5–15
20. Shalu, Chaurasia S.K., Singh R.K., Chandra S., Electrical, mechanical, structural, and thermal behaviours of polymeric gel electrolyte membranes of poly(vinylidene fluoride-co-hexafluoropropylene) with the ionic liquid 1-butyl-3-methylimidazolium tetrafluoroborate plus lithium tetrafluoroborate, Journal of Applied Polymer Science, 132, 7(2015)
21. Liu W., Niu T., Yang J., Wang Y., Hu S., Dong Y., Xu H., Preparation of micronsized alumina powders from aluminium beverage can by means of sol–gel process ,Micro & Nano Letters, 10(2011), 852 –854
22. Hong-bin Tan., Preparation of long alumina fibers by sol-gel method using tartaric acid, International Journal of Minerals Metallurgy and Materials, 12(2011)
23. Saleh T., Gupta V., Characterization of the Chemical Bonding between Al_2O_3 and Nanotube in MWCNT/Al_2O_3 Nanocomposite, Current Nanoscience, 5(2012)
24. Yilmaz S., Kalpakli Y., Yilmaz E., Synthesis and characterization of boehmitic alumina coated graphite by sol–gel method. Ceramics International, 5(2009), 2029–2034
25. Pathak L.C., Singh T.B, Verma A.K., Ramachandrarao P., Synthesis of nano-crystalline alumina powder by Sol-gel Process. Journal of Metallurgy and materials Science, 42 (2000), 93-104.
26. Alex T.C., An insight into the changes in the thermal analysis curves of boehmite with mechanical activation. Journal of Thermal Analysis and Calorimetry, 117 (2014) 163-171.
27. Tan H.,Preparation of long alumina fibers by sol-gel method using malic acid, International Journal of Minerals Metallurgy and Materials, 7(2011), 1563-1567.
28. Petrakli F., Dimitris S., Athena T., Development of Highly Dispersed Hybrid Nanoalumina with the Sol- Gel Method, Advances in Science and Technology, 2014.

29. Mirjalili F., Hasmaliza M., Chuah Abdullah L., Size-controlled synthesis of nano α-alumina particles through the sol–gel method, Ceramics International, 36 (2010), 1253-1257
30. Rogojan R., Andronescu E., Ghiţulică C., Vasile B., Synthesis and characterization of alumina nano-powder obtained by sol-gel method, U.P.B. Science Bulletin, 73(2011), 68-76
31. Liu H., Ning G., Gan Z., Lin Y., A simple procedure to prepare spherical α-alumina powders, Materials Research Bulletin, 44(2009), 785-788
32. Zhu H.X., Liu S.K., Mechanical properties of squeeze-cast zinc alloy matrix composites containing α-alumina fibres, Composites, 5(1993), 437–442
33. Genel K., Kurnaz S.C., Durman M., Modeling of tribological properties of alumina fiber reinforced zinc–aluminum composites using artificial neural network, Materials Science and Engineering: A, 363(2003), 203–210
34. Arikan R., Murphy S., Anisotropic wear of planar-random metal matrix composites with zinc alloy matrix, Wear, 143(1991), 149–157
35. Prasad B.K., Effects of alumina particle dispersion on the erosive–corrosive wear response of a zinc-based alloy under changing slurry conditions and distance, Wear, 238(2000), 151–159
36. Modi O.P., Rathod S., Prasad B.K., Jha A.K., Dixit G., The influence of alumina particle dispersion and test parameters on dry sliding wear behaviour of zinc-based alloy, Tribology International, 40 (2007), 1137–1146
37. Matteazzi P., Caër G., Synthesis of Nanocrystalline Alumina–Metal Composites by Room-Temperature Ball-Milling of Metal Oxides and Aluminium, 75(1992), 2749–2755

.....